UCLA
UCLA Electronic Theses and Dissertations

Title
Fractional Optimal Control Via Spectral Factorization

Permalink
https://escholarship.org/uc/item/9047d880

Author
Zhou, Bonan

Publication Date
2019

Peer reviewed|Thesis/dissertation

UNIVERSITY OF CALIFORNIA

Los Angeles

Fractional Optimal Control Via Spectral Factorization

A dissertation submitted in partial satisfaction of the

requirements for the degree Doctor of Philosophy

in Aerospace Engineering

by

Bonan Zhou

2019

ABSTRACT OF THE DISSERTATION

Fractional Optimal Control Via Spectral Factorization

by

Bonan Zhou

Doctor of Philosophy in Aerospace Engineering

University of California, Los Angeles, 2019

Professor Jason L. Speyer, Chair

The spectral factorization solution for fractional order optimal control problems is provided. First, graphical tools are used to obtain stabilizing controllers as well as derive properties of fractional polynomials. Second, the spectral factorization solution to the output feedback $\mathscr{H}_2$ problem is extended to fractional systems, which are permitted to be unstable, non-minimum phase, or incommensurate order. Third, spectral factorization is used to solve the LQR problem of constructing the optimal full-state feedback law, which is shown to have strong connections to the rational LQR.

The dissertation of Bonan Zhou is approved.

Robert T. M'Closkey

Elisa Franco

Mario Bonk

Jason L. Speyer, Committee Chair.

University of California, Los Angeles

2019

Contents

List of Figures

M.S., UCLA, Aerospace Engineering, 2016.

B.S., UCLA, Physics, 2010.

1 Introduction

This work is on the solution of fractional optimal control problems via spectral factorization. As the need to model complex systems has arisen, interest in fractional differential equations has increased. Fractional differential equations are now used to model memory phenomena such as viscoelasticity and fractances [10, 14]. These phenomena share a common physical origin: a microscopic fractal structure, which manifests macroscopically as hysteresis [10, 14]. While this description perhaps suggests the obscure or exotic, to the contrary, fractional systems are mundane. Nature is replete with fractal structures, where small elements, such as cells, pores, or grains, are embedded in a nested, self-similar hierarchy. Despite their ubiquity in nature, fractional systems have only recently caught the attention of control theorists. This is likely due to the desire to engineer artifical systems that are inspired by or directly incorporate nature. For instance, fractional control has found applications in flexible structures and soft robotics [10, 14]. Moreover, even when the dynamics of interest are Newtonian, there is often the need to reject noise processes generated by fractional systems. A common example is flicker noise, with its signature $1/\omega$ spectrum. Yet, despite the commonality of fractional systems, fractional control theory is far from mature. Because fractional differential equations have primarily been the purview of mathematicians, many problems that are of interest to control theorists have received limited attention. One of the most significant of these problems is that of frequency domain optimal control of fractional systems.

Linear time-invariant fractional differential equations have the form,

$$\sum a_i \mathscr{D}^{\alpha_i} y(t) = \sum b_j \mathscr{D}^{\beta_j} u(t), \tag{1}$$

where $y(t)$ is the output, $u(t)$ is the input, $a_i, b_j \in \mathscr{R}$, and $\alpha_i, \beta_j \in \mathscr{R}^+$. There are three definitions of the fractional derivative [10, 14] which we briefly summarize. First, the Riemann-Liouville derivative is the composition of the integer derivative and fractional integeral, which is a generalization of the formula for repeated integrations,

$$\mathscr{D}_R^\alpha y(t) = \frac{d^m}{dt^m} \frac{1}{\Gamma(m-\alpha)!} \int_0^t (t-\tau)^{m-\alpha-1} y(\tau) d\tau. \tag{2}$$

where $\alpha \in [m-1, m]$ and $m \in \mathscr{Z}^+$. Second, the Caputo derivative switches the order of the fractional

integral and integer derivative,

$$\mathscr{D}_C^\alpha y(t) = \frac{1}{\Gamma(m-\alpha)!} \int_0^t (t-\tau)^{m-\alpha-1} \frac{d^m y}{dt^m}\bigg|_{t=\tau} d\tau. \tag{3}$$

Third, the Grunwald-Letnikov derivative is the fractional generalization of the formula for repeated differentiations,

$$\mathscr{D}_L^\alpha y(t) = \lim_{\Delta t \to 0} \frac{\sum_{k=0}^\infty \binom{\alpha}{k}(-1)^k y(t + (\alpha-k)dt)}{\Delta t^\alpha}, \tag{4}$$

where

$$\binom{\alpha}{k} = \frac{\Gamma(\alpha+1)}{k!\Gamma(\alpha-k+1)}. \tag{5}$$

The difference between these fractional derivatives is most apparent when one considers their Laplace transforms.

The Laplace transforms of these fractional derivatives [10, 14] are

$$\mathscr{L}(\mathscr{D}_R^\alpha y(t)) = s^\alpha Y(s) - \sum_{k=0}^{m-1} s^k [\mathscr{D}_R^{\alpha-k-1} y(t)]_{t=0}, \tag{6}$$

$$\mathscr{L}(\mathscr{D}_C^\alpha y(t)) = s^\alpha Y(s) - \sum_{k=0}^{m-1} s^{\alpha-k-1} y^{(k)}(0), \tag{7}$$

$$\mathscr{L}(\mathscr{D}_L^\alpha y(t)) = s^\alpha Y(s). \tag{8}$$

The Riemann-Liouville derivative was the original definition of fractional differentiation, but is mostly of interest to mathematicians due to its dependence on fractional order initial conditions. The Caputo derivative is favored in applications due to its dependence on integer order initial conditions. The Grunwald-Letnikov derivative assumes zero initial conditions, but is useful for constructing fractional difference equations in discrete time.

In this work, we are interested in frequency domain optimal control, which concerns properties of the steady-state. Thus, for our purposes, we do not distinguish between these definitions since the varying treatment of the initial conditions is irrelevant. As indicated by their amenability to the Laplace transform, the frequency domain is a natural setting for the study of fractional systems. Unlike rational systems, fractional systems are infinite dimensional and do not possess a well-defined state-space [10]. Consequently, one of the greatest advantages of the time-domain, the alebraic unification of single-input, single-output systems and multiple-input, multiple-output systems, is lost when considering fractional systems. On the

other hand, the input-output relationships themselves are perfectly well-defined. Therefore, we reduce our study of fractional differential equations to the study of *fractional transfer functions*.

Fractional transfer functions are the mapping, $P(s) = Y(s)/U(s)$,

$$P(s) = \frac{\sum b_j s^{\beta_j}}{\sum a_i s^{\alpha_i}}. \tag{9}$$

The numerator and denominator of $P(s)$ are termed *fractional polynomials*. Fractional polynomials are polynomial-like functions that are multi-valued due to the non-integer exponents of s. Because they are multi-valued, fractional polynomials are only analytically continuous for $\arg(s) \in (-\pi, \pi)$. In other words, each term with a fractional exponent is discontinuous across the negative real-axis. To resolve the discontinuity, we restrict the domain to $s \in \mathscr{C}/\mathscr{R}^-$, which is a subset of the complex plane known as the primary Riemann sheet or *slit s-plane*. This is equivalent to placing a *branch cut* along the negative real-axis, which forbids any line of analytic continuity from crossing it. Fractional polynomials are thus imbued with singularities at the origin known as *branch points*.
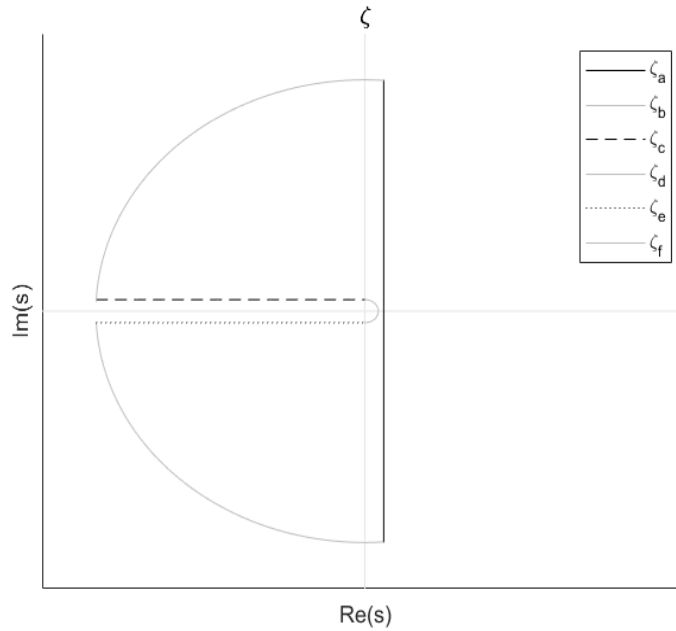
Figure 1: Contour $\zeta = \zeta_a + \zeta_b + \zeta_c + \zeta_d + \zeta_e + \zeta_f$.

The branch cut and associated branch points have strong consequences for the inverse Laplace transform,

3

$$y(t) = \mathcal{L}^{-1}(Y(s)),$$

$$\mathcal{L}^{-1}(Y(s)) = \frac{1}{2\pi i} \int_{-i\infty}^{i\infty} Y(s) \exp(st) ds. \tag{10}$$

Normally, the inverse Laplace transform is calculated with the Residue Theorem, which states that the integral around around a closed contour evaluates to the sum of the residues of the poles, p_j, within the contour,

$$\oint Y(s) \exp(st) ds = 2\pi i \sum \lim_{s \to p_j} (s - p_j) Y(s) \exp(st). \tag{11}$$

However, the branch cut prevents us from invoking any contour that crosses the negative real-axis. Thus, we use the slit contour, ζ, as shown in Fig. 1. We then subdivide the contour integral as

$$I_i = \int_{\zeta_i} Y(s) \exp(st) ds. \tag{12}$$

From the Residue Theorem,

$$I_a + I_b + I_c + I_d + I_e + I_f = 2\pi i \sum \lim_{s \to p_j} (s - p_j) Y(s) \exp(st). \tag{13}$$

The integral we are interested in is

$$\frac{1}{2\pi i} I_a = \mathcal{L}^{-1}(Y(s)). \tag{14}$$

Along ζ_c and ζ_e, we use the respective parameterizations, $s = \rho \exp(i\pi)$ and $s = \rho \exp(-i\pi)$, where $\rho > 0$, resulting in

$$\frac{1}{2\pi i} (I_c + I_e) = -\frac{1}{\pi} \Im \left[\int_0^\infty Y(-\rho) \exp(-\rho t) d\rho \right]. \tag{15}$$

As $|\zeta_b|, |\zeta_f| \to \infty$, $I_b, I_f \to 0$. As $|\zeta_d| \to 0$, $I_d \to 0$. Hence,

$$\mathcal{L}^{-1}(Y(s)) = \frac{1}{\pi} \Im \left[\int_0^\infty Y(-\rho) \exp(-\rho t) d\rho \right] + \sum \lim_{s \to p_j} (s - p_j) Y(s) \exp(st). \tag{16}$$

The term in square brackets is the unique contribution of the branch points to the time domain response. Since the branch points correspond to a monotonically decreasing function of time [10], we refer to the branch points of fractional polynomials and transfer functions as stable. Consequently, the stability properties of a fractional system depend entirely on the poles. Just as for rational systems, fractional transfer functions are stable if all poles are in the LHP (left-half plane) and unstable if there are any poles in the RHP (right-half plane).

Branch points complicate the application of *Wiener-Hopf spectral factorization.* Wiener-Hopf spectral factorization or simply, spectral factorization, is a frequency domain technique for obtaining solutions to integral minimization problems [4, 6, 7, 13, 15, 18]. The key step is a factorization of the form,

$$|f_1|^2 + |f_2|^2 = [|f_1|^2 + |f_2|^2]^+ [|f_1|^2 + |f_2|^2]^-, \tag{17}$$

where f_1 and f_2 are fractional polynomials related to the numerator and denominator of the plant, and $[.]^+$ and $[.]^-$, are the stable and unstable multiplicative factors of $[.]$. While the branch points of $f_1 = f_1(s)$ and $f_2 = f_2(s)$ are stable, the branch points of $\bar{f}_1 = f_1(-s)$ and $\bar{f}_2 = f_2(-s)$ are unstable. Thus, $|f_1|^2 + |f_2|^2$ contains both stable and unstable branch points, which must be factored in addition to the roots.

The paucity of literature on fractional optimal control using spectral factorization is likely explained by the difficulty of the desired factorization. The only prior work that has addressed fractional optimal control using spectral factorization method is that of Vinagre and Feliu [16]. They studied factorizations satisfying the following special condition: f_1 and f_2 share a common minimum-phase stable fractional factor, μ, such that $f_1 = \mu z_1$, $f_2 = \mu z_2$, where z_1 and z_2 are polynomials formed by the product of the RHP roots of f_1 and f_2, respectively. When this condition holds, the fractional factorization reduces to an elementary polynomial factorization:

$$[|f_1|^2 + |f_2|^2]^+ = [|\mu|^2]^+ [|z_1|^2 + |z_2|^2]^+ = \mu[|z_1|^2 + |z_2|^2]^+. \tag{18}$$

$$[|f_1|^2 + |f_2|^2]^- = [|\mu|^2]^- [|z_1|^2 + |z_2|^2]^- = \bar{\mu}[|z_1|^2 + |z_2|^2]^-. \tag{19}$$

Since $\mu = f_1/z_1 = f_2/z_2$, all the stable branch points are contained in μ, whereas all the unstable branch points are contained in $\bar{\mu}$. However, the condition that f_1 and f_2 share this common factor, μ, is quite unusual. Perhaps recognizing the narrowness of this special condition, Vinagre and Feliu provide two examples of a tracking system where there is no penalty on the control effort, in which case $f_2 = 0$. Thus, the desired factorization assumes an especially simple form,

$$[|f_1|^2]^+ = \mu\bar{z}_1, \tag{20}$$

$$[|f_1|^2]^- = \bar{\mu}z_1. \tag{21}$$

In the general case when $f_1 \neq \mu z_1$, $f_2 \neq \mu z_2$, the factorization is far more difficult. Counterintuitively, knowledge of the roots of $|f_1|^2 + |f_2|^2$ is insufficient to perform the factorization. To illustrate, suppose we

define z to be the polynomial formed by the product of the RHP roots of $|f_1|^2 + |f_2|^2$. Consider an attempt to factor $|f_1|^2 + |f_2|^2$ using z:

$$[|f_1|^2 + |f_2|^2]^+ = [\frac{|f_1|^2 + |f_2|^2}{|z|^2}|z|^2]^+ = [\frac{|f_1|^2 + |f_2|^2}{|z|^2}]^+ \bar{z}. \tag{22}$$

$$[|f_1|^2 + |f_2|^2]^- = [\frac{|f_1|^2 + |f_2|^2}{|z|^2}|z|^2]^- = [\frac{|f_1|^2 + |f_2|^2}{|z|^2}]^- z. \tag{23}$$

While the term, $(|f_1|^2 + |f_2|^2)/|z|^2$, does not contain simple poles or zeros, it retains both its stable and unstable branch points. Thus, an elementary decomposition of the branch points does not follow:

$$[\frac{|f_1|^2 + |f_2|^2}{|z|^2}]^+ \neq \mu, \tag{24}$$

$$[\frac{|f_1|^2 + |f_2|^2}{|z|^2}]^- \neq \bar{\mu}. \tag{25}$$

Suffice it to say, the chief obstacle to frequency domain optimal control of fractional systems is treatment of this general class of fractional product decompositions.

While the objective is to solve fractional optimal control problems with spectral factorization, a precursor for optimality is stability. Thus, this work is organized as follows. We begin by deriving several results related to the roots of fractional polynomials. Concurrently, we discuss the use of classical control techniques such as the root locus to obtain stabilizing controllers for fractional systems. These tools will be useful when we solve the fractional $\mathscr{H}_2$ problem of constructing the optimal output feedback controller, which requires knowledge of a nominal stabilizing controller. It is here that we generalize the Wiener-Hopf spectral factorization technique to fractional systems. Finally, we use this generalized factorization technique to solve the fractional LQR (linear quadratic regulator) problem, which has a surpising symmetry with the rational LQR and elucidates the meaning of the optimal output feedback controller.

2 Fractional Stability

Stability of fractional transfer functions depends on the location of the poles. Thus, we are interested in the roots of fractional polynomials. In general, fractional polynomials are transcendental functions so the roots cannot be calculated algebraically. However, if a fractional polynomial becomes a polynomial under the transformation, $s = \nu^r$, where $r \in \mathscr{R}^+$, then the roots can be solved for in the ν-plane. The roots that appear in the s-plane are simply those in the sector, $r \arg(\nu) \in (-\pi, \pi)$. This leads to the distinction between fractional transfer functions of *commensurate* and *incommensurate* order [10]. Commensurate order transfer functions can be transformed into rational transfer functions in a mapping plane, whereas incommensurate order transfer functions cannot. Unsurprisingly, fractional systems research is often restricted to commensurate order systems because the poles and zeros can be calculated algebraically. Since fractional exponents are ultimately approximated to finite precision on a digital computer, fractional systems are reducible to commensurate order systems, in a practical sense.

Nevertheless, the relative algebraic facility of commensurate order systems is not as useful as one might think. Consider the incommensurate order transfer function,

$$P(s) = \frac{1}{s^{\sqrt{3}} + s^{\sqrt{2}} + s + 1}. \tag{26}$$

The irrational exponents are meant to represent the results of a fitting procedure with high-precision. Suppose one instead used the commensurate order approximation,

$$P(s) = \frac{1}{s^{1.73} + s^{1.41} + s + 1}. \tag{27}$$

With this approximation, the mapping $s = \nu^{100}$ results in a 173rd order rational transfer function in ν-plane. While high order systems are not necessarily a problem for a computer, they are a problem for reasoning about fractional systems qualitatively. Not all 173 ν-plane roots matter; in fact, only 2 of them actually appear on the s-plane. Certainly, one could truncate the precision of the exponents further. However, a less arbitrary approach is to analyze fractional transfer functions directly on the s-plane. In so doing, we gain insights into fractional dynamics that would otherwise remain opaque.
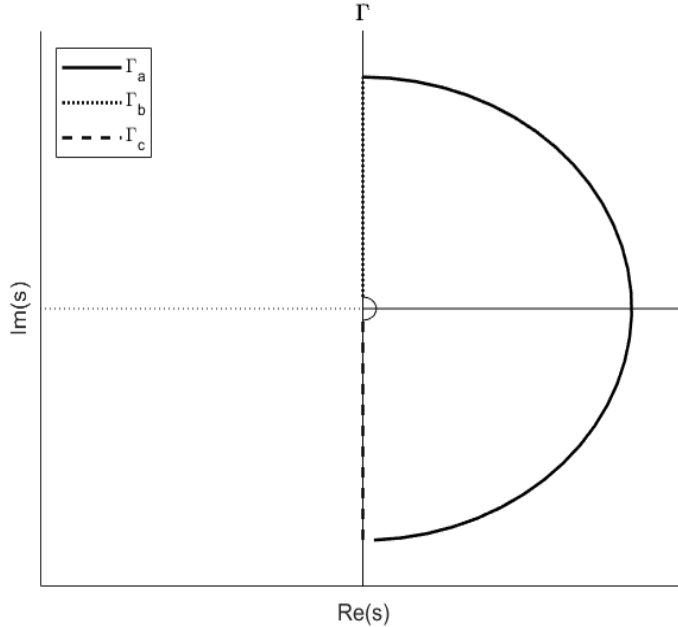
Figure 2: Contour $\Gamma = \Gamma_a + \Gamma_b + \Gamma_c$.

2.1 Argument Principle

Our starting point is the Argument Principle, and relatedly, the Nyquist stability criterion. The Argument Principle may be applied to fractional systems almost exactly the same way that it is applied to rational systems. The only difference is that the traditional contour enclosing the RHP must avoid the branch points at the origin. Thus, to determine the stability of a fractional polynomial, $f(s)$, we use the contour, $\Gamma = \Gamma_a + \Gamma_b + \Gamma_c$ (Fig. 2). The winding number,

$$W(f(\Gamma), 0) = \frac{\Delta \arg f(\Gamma)}{2\pi}, \tag{28}$$

is the number of roots of f in the RHP of the slit s-plane [3]. To check the stability of an arbitrary fractional polynomial, this graphical condition can always be examined. Of course, as $|s| \to \infty$, $f(s) \to \infty$. Thus, a simple improvement is to use the Argument Principle with respect to the normalized function,

$$A(s) = \frac{f(s)}{(s^\delta + 1)^m}, \tag{29}$$

8

where $\delta \in [1, 2)$, $m = \lfloor \alpha \rfloor$, and $\alpha = m\delta$. By construction, $A(s)$ has no RHP poles. Hence, we may equate the winding numbers,

$$W(f(\Gamma), 0) = W(A(\Gamma), 0). \tag{30}$$

As $|s| \to \infty$, $A(s)$ is bounded. Thus, it is more convenient to consider $W(A(\Gamma), 0)$. However, the following theorem shows that in some cases, even this is unnecessary.

Theorem 2.1. *If a fractional polynomial, $f(s)$, satisfies $\alpha = \max_i \alpha_i \leq 2$ and $a_i > 0$, then $f(s)$ is stable.*

Proof. The winding number is

$$W(f(\Gamma), 0) = \frac{\Delta \arg f(\Gamma_a)}{2\pi} + \frac{\Delta \arg f(\Gamma_b + \Gamma_c)}{2\pi}. \tag{31}$$

Along Γ_a, we use the parameterization $s = \rho \exp(i\phi)$, where $\rho \to \infty$ and $\phi \in [-\pi/2, \pi/2]$, resulting in

$$\frac{\Delta \arg f(\Gamma_a)}{2\pi} = \frac{\Delta \arg f(\rho \exp(i\phi))}{2\pi} = \frac{\alpha}{2} \leq 1. \tag{32}$$

To bound $\Delta \arg f(\Gamma_b + \Gamma_c)$, we note that because the image of $f(\Gamma_c)$ is the reflection of the image of $f(\Gamma_b)$ about the real-axis, it suffices to examine the real-axis intercepts of $f(\Gamma_b)$. Along Γ_b, we use the parameterization, $s = i\omega$, where $\omega \in (0, \infty)$. The number of real-axis intercepts (excluding the intercept at $\omega = 0$) is the number of positive real roots of $\Im[f(i\omega)]$, where

$$\Im[f(i\omega)] = \sum a_i \sin(\frac{\alpha_i \pi}{2}) \omega^{\alpha_i}. \tag{33}$$

If $\alpha \leq 2$ and $a_i > 0$, then $\Im[f(i\omega)]$ has no sign changes i.e. is strictly positive for $\omega > 0$. Therefore, $\Im[f(i\omega)]$ has no positive real roots. Consequently, neither $f(\Gamma_a)$ nor $f(\Gamma_b + \Gamma_c)$ crosses the real-axis except when $\omega = 0$. Noting that the real-intercept is on the positive real-axis, that the image of $f(\Gamma)$ is continuous, and that $\Delta \arg(f(\Gamma_a)) > 0$,

$$\frac{\Delta \arg f(\Gamma_b + \Gamma_c)}{2\pi} < 0. \tag{34}$$

Combining bounds,

$$W(f(\Gamma), 0) \leq 1 + \frac{\Delta \arg f(\Gamma_b + \Gamma_c)}{2\pi}. \tag{35}$$

Since the winding number of a function without poles is a non-negative integer,

$$W(f(\Gamma), 0) = 0. \tag{36}$$

9

□

Theorem 2.1 has an intuitive physical interpretation. Second-order fractional polynomials with positive coefficients correspond to generalized Newtonian systems with only fractional friction forces. Since these forces only dissipate energy, such systems must be stable. For example, examining the plants (26), (27), we see without any calculation that these plants are stable.

The Nyquist stability criterion follows from the Argument Principle straightforwardly. To determine the stabilty of the closed-loop denominator,

$$1 + kP, \tag{37}$$

we examine the winding number,

$$W(kP(\Gamma), -1), \tag{38}$$

which is equivalent to the number of closed-loop poles minus the number of open-loop poles. Of course, it is possible to rely on the Argument Principle and Nyquist stability criterion to determine stability of the open and closed-loop. However, it is often helpful in controller design to have a direct visualization of the location of the closed-loop poles themselves. This is the technique of the root locus, which is the subject of the next section.

2.2   Root Locus

The original purpose of the root locus was to serve as a graphical aid to design controllers for unstable or neutrally stable systems where the loopshaping approach is difficult [8]. For fractional systems, the root locus is more important than it normally is for rational systems due to the lack of general algebraic stability criteria [10]. The root locus of $P(s)$ is those values of s satisfying $1 + kP(s) = 0$ as $k \in \mathscr{R}$ is varied. In prior discussions, the assumption has always been to approximate the fractional transfer function with a commensurate order one, and then construct the rational locus in the ν-plane, adjusting the interpretation of the stability region accordingly [10]. However, if the equivalent rational function in ν is high-order, then this defeats the purpose of the locus, which is to be an intuitive control design tool. In contrast, our approach is to construct the fractional locus on the slit s-plane. As we will show, the advantage of this approach is that no matter how many critical frequencies there are on the entire Riemann surface, the number of

10

critical frequencies on the primary Riemann sheet is comparably small. Consequently, the fractional locus on the primary Riemann sheet is not only easier to construct and interpret, but more useful for preliminary controller design.

To construct the locus, we require knowledge of its features for both small and large k. This allows us to estimate its overall structure from continuity. Because our goal is stability, rough knowledge of the locus is sufficient to gauge the plausibility of a nominal stabilizing controller. We begin by deducing basic features of the locus. We can see that as the magnitude of k increases, branches of the fractional locus still extend from the open-loop poles to the open-loop zeros. Because we consider only fractional transfer functions with real coefficients, the fractional locus is still symmetric about the real-axis, via the Reflection Principle [3]. On the other hand, the fractional locus cannot lie on the negative real-axis, as this is by definition, not on the slit s-plane. However, the locus can still lie on the positive real-axis to the left of an odd number of poles and zeros.

We now analyze the asymptotes of the locus. As $|s| \to \infty$, $P(s) \to s^{\beta - \alpha}$, where $\alpha = \max_i \alpha_i$ and $\beta = \max_j \beta_j$. If k is positive, then for $n = 1, 2, 3...$, the asymptote angles, ϕ, are

$$\phi = \pm \frac{(2n-1)\pi}{\alpha - \beta}. \tag{39}$$

Then, since roots on the slit s-plane satisfy $\arg(s) \in (-\pi, \pi)$, the number of asymptotes that lie on the slit s-plane, N_a, is

$$N_a = 2 \lfloor \frac{\alpha - \beta + 1}{2} \rfloor. \tag{40}$$

If k is negative, then for $n = 1, 2, 3...$, the asymptote angles are

$$\phi = \pm \frac{(2n-2)\pi}{\alpha - \beta}. \tag{41}$$

Thus, the number of asymptotes is instead

$$N_a = 2 \lfloor \frac{\alpha - \beta}{2} \rfloor + 1. \tag{42}$$

This case of negative k will be important in the next section, when we bound the number of roots of a fractional polynomial on the slit s-plane.

From the number of zeros, n_z, and number of asymptotes, N_a, we can deduce the number of branches of the locus, N_b, which we define as those branches that remain on the slit s-plane as $k \to \infty$. It must hold

11

that for each open-loop zero, there will be an arriving pole as $k \to \infty$. However, it must also hold that for each asymptote, there will be a departing pole as $k \to \infty$. Therefore, to simultaneously satisfy both of these requirements, the number of branches must be

$$N_b = n_z + N_a. \tag{43}$$

For a rational transfer function, $N_a = n_p - n_z$, where n_p is the number of open-loop poles. Hence, for a rational transfer function, $N_b = n_z + n_p - n_z = n_p$. However, for a fractional transfer function, $N_a \neq n_p - n_z$, in general. Consequently,

$$N_b \neq n_p. \tag{44}$$

Thus, if there is a discrepancy between N_b and n_p, then *additional poles will either enter or leave the slit s-plane by crossing the branch cut.*

Lastly, we consider the departure angles (note that the arrival angles follow almost identically). We begin with the case of a simple pole at $-p$ of multiplicity m. From L'Hôpital's rule,

$$g(-p) = \lim_{s \to -p} \arg \frac{\sum a_i s^{\alpha_i}(s)}{(s+p)^m}, \tag{45}$$

is a non-zero constant. Hence, for $n = 1, 2, 3...$, the departure angles, $\psi \in (-\pi, \pi)$, are

$$m\psi = \pm(2n-1)\pi + \arg \sum b_j(-p)^{\beta_j} - \arg g(-p). \tag{46}$$

We now consider the case of a fractional pole of the form $(s + \rho)^\eta$ where $\rho, \eta \in \mathscr{R}^+$. Here, the numerator of the plant can be written

$$\sum a_i s^{\alpha_i} = h(s)(s+\rho)^\eta. \tag{47}$$

In this case, $s = -\rho$ is technically not a pole as it lies on the branch cut, which is not part of the slit s-plane. However, this fractional pole will still have departure angles, $\psi \in (-\pi, \pi)$,

$$\eta\psi = \pm(2n-1)\pi + \arg \sum b_j(-\rho)^{\beta_j} - \arg h(-\rho), \tag{48}$$

where $h(-\rho)$ is a non-zero constant. These departure angles are especially relevant when analyzing neutrally stable fractional systems.

In addition to assisting controller design, the locus may be more broadly construed as a tool for analyzing the roots of fractional polynomials. In fact, the locus combined with the Argument principle can be used to deduce helpful bounds on the number of roots of fractional polynomials.

2.3 Properties of Fractional Polynomials

Here we derive properties of fractional polynomials,

$$f(s) = \sum a_i s^{\alpha_i}, \tag{49}$$

where the exponents are ordered such that $\alpha_i > \alpha_{i-1}$. It is well-known for polynomials that the number of positive real roots is bounded by the number of consecutive sign changes. This property obviously extends to commensurate order fractional polynomials, because the slit s-plane and the ν-plane share the same positive real-axis. However, we can use the locus to show that this *rule of signs* also extends to incommensurate fractional polynomials.

Lemma 2.2. *The number of positive real roots, $N_r(f(s))$, satisfies*

$$N_r(f(s)) \leq N_s(f(s)), \tag{50}$$

where $N_s(f(s))$ is the number of consecutive sign changes between terms of $f(s)$.

Proof. We recursively express $f(s)$ as

$$f_i(s) = a_i s^{\alpha_i} + f_{i-1}(s). \tag{51}$$

The roots of $f_i(s)$ are points on the root locus of

$$1 + \frac{f_{i-1}(s)}{a_i s^{\alpha_i}} = 1 + \frac{a_{i-1} s^{\alpha_{i-1}} + f_{i-2}(s)}{a_i s^{\alpha_i}} = 0, \tag{52}$$

with respect to a_i^{-1}. A necessary condition for a positive real root departing to $+\infty$ is if there is an asymptote with $\phi = 0$. Comparing (39) and (41), we see that $\phi = 0$ if and only if a_i and a_{i-1} have opposite sign. Consequently, the number of positive real roots, $N_r(f_i(s))$, is at most one positive real root departing to $+\infty$ plus any positive real roots of $f_{i-1}(s)$. Therefore,

$$N_r(f_i(s)) \leq N_r(f_{i-1}(s)) + I_i, \tag{53}$$

13

where I_i is an indicator function such that $I_i = 0$ if a_i and a_{i-1} have the same sign and $I_i = 1$ if a_i and a_{i-1} have opposite sign. This bound becomes sharp if a_i is sufficiently small. Solving for the recursion,

$$N_r(f(s)) \leq \sum I_i, \tag{54}$$

where $\sum I_i = N_s(f(s))$. $\square$

Lemma 2.2 is useful for bounding the total number of roots of a fractional polynomial on the slit s-plane. It is well-known that for commensurate order fractional polynomials, that the roots satisfying $r \arg(\nu) \in (-\pi, \pi)$ in the ν-plane will be the roots that are mapped to the slit s-plane. The maximum number of roots in s is achieved when all of the roots in ν lie in this sector. Thus, the maximum number of roots in s is the order of the polynomial in ν. However, for incommensurate order fractional polynomials, this algebraic argument cannot be made. Instead, we use the Argument Principle in conjunction with a contour that encloses the slit s-plane, infinitesimally avoiding the branch cut. Thus, to bound the number of roots of a fractional polynomial, $f(s)$, we use the contour, $\tau = \tau_a + \tau_b + \tau_c$ (Fig. 3). The winding number,

$$W(f(\tau), 0) = \frac{\Delta \arg f(\tau)}{2\pi}, \tag{55}$$

is the number of roots on the slit s-plane.

Theorem 2.3. *The number of roots of a fractional polynomial, $f(s)$, on the primary Riemann sheet, $W(f(\tau), 0)$, is bounded by*

$$W(f(\tau), 0) < \alpha + N_s(\Im[f(-\rho)]) + 1, \tag{56}$$

where $\rho \in \mathscr{R}^+$. If $a_i > 0$, then

$$W(f(\tau), 0) \leq 2\lfloor \alpha \rfloor. \tag{57}$$

Proof. The winding number has the upper bound,

$$W(f(\tau), 0) \leq \left| \frac{\Delta \arg f(\tau_a)}{2\pi} \right| + \left| \frac{\Delta \arg f(\tau_b + \tau_c)}{2\pi} \right|, \tag{58}$$

which becomes sharp if the changes in argument have the same sign. Along τ_a, we use the parameterization, $s = \rho \exp(i\phi)$, where $\rho \to \infty$ and $\phi \in (-\pi, \pi)$, resulting in

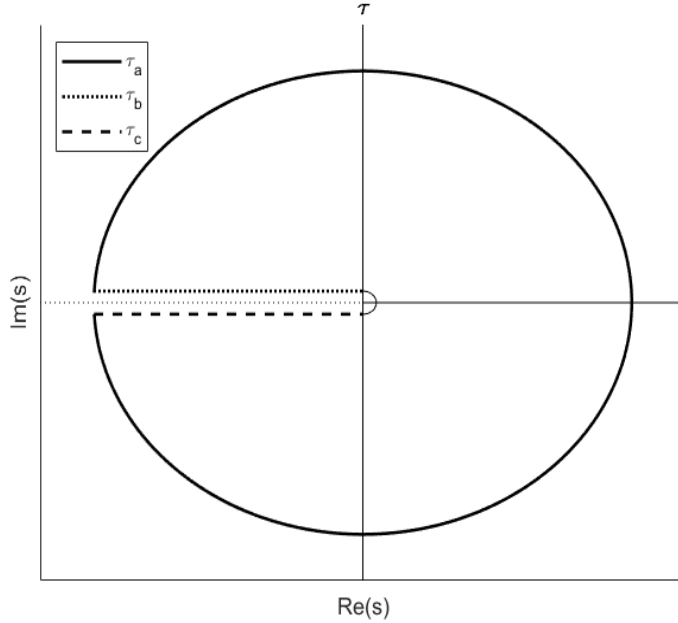$$\frac{\Delta \arg f(\tau_a)}{2\pi} = \frac{\Delta \arg f(\rho \exp(i\phi))}{2\pi} = \alpha - \epsilon, \tag{59}$$

Figure 3: Contour $\tau = \tau_a + \tau_b + \tau_c$.

where $\alpha = \max_i \alpha_i$ and $\epsilon \to 0^+$. We denote the unsigned whole number of encirclements of $f(\tau_b + \tau_c)$ around the origin as N_{bc}. The change in argument of $f(\tau_b + \tau_c)$ is bounded by

$$\frac{\Delta \arg f(\tau_b + \tau_c)}{2\pi} < N_{bc} + 1. \tag{60}$$

We can bound N_{bc} with the number of real-axis intercepts of $f(\tau_b)$. We denote each of these intercepts as σ_i. The image of $f(\tau_b)$ is a continuous curve passing through each σ_i once. The image of $f(\tau_c)$ is the reflection of the image of $f(\tau_b)$ about the real axis and, consequently, also passes through each σ_i once. Therefore, we can associate each encirclement counted in N_{bc} with a pair of intercepts σ_i, σ_{i-1} where the last intercept, σ_0, corresponds to $\rho = 0$. Along τ_b, we use the parameterization, $s = -\rho$, where $\rho \in (0, \infty)$. The number of intercepts (excluding σ_0) is the number of positive real roots, $N_r(\Im[f(-\rho)])$. Noting that the intercepts do not necessarily define concentric encirclements,

$$N_{bc} \leq N_r(\Im[f(-\rho)]). \tag{61}$$

Since $\Im[f(-\rho)]$ is a fractional polynomial in ρ, we can apply Lemma 2.2 to obtain the bound

$$N_r(\Im[f(-\rho)]) \leq N_s(\Im[f(-\rho)]). \tag{62}$$

15

Combining bounds, we obtain (56). This bound simplifies further if the coefficients of $f(s)$ are positive. The fractional polynomial, $\Im[f(-\rho)]$, has the form

$$\Im[f(-\rho)] = \sum a_i \sin(\alpha_i \pi) \rho^{\alpha_i}. \tag{63}$$

From the periodicity of $\sin(\alpha_i \pi)$,

$$N_s(\Im[f(-\rho)]) \le \lfloor \alpha \rfloor. \tag{64}$$

Hence, the bound becomes

$$W(f(\tau), 0) < \alpha + \lfloor \alpha \rfloor + 1. \tag{65}$$

Since $f(s)$ is symmetric with respect to the real-axis, and has neither positive real roots (due to the positive coefficients) nor negative real roots (due to the branch cut), $W(f(\tau), 0)$ must be an even number, resulting in (57). $\qquad \square$

For fractional polynomials with only positive coefficients, one obtains a bound that depends only on the order of the highest term, analogous to the Fundamental Theorem of Algebra for polynomials. Together, (56) and (57) explain why the number of roots of a fractional polynomial on the slit s-plane is guaranteed to be small compared to the number of roots in the ν-plane; the number of roots is related to the highest order term and number of terms, not the finite precision of the exponents, which is an artifact of the ν-plane approach.

2.4 Examples

In the following examples, we design stabilizing controllers for fractional plants. We estimate the fractional locus by calculating the asymptote angles (39), number of asymptotes (40), number of branches (43), and when relevant, departure angles (48). Note that the fractional loci depicted in the figures are obtained via numerical solution of the roots of the closed-loop denominator. These require some effort to generate and are presented only for the sake verifying the approximate loci one would construct using the aforementioned rules.

2.4.1 Example

Consider the plant

$$P(s) = \frac{s^{\sqrt{7}} + 10s^{\sqrt{2}} + 50}{s^{\sqrt{14}} + 5}, \tag{66}$$

The poles are at $s \approx 1.0266 \pm 1.1445i, -1.2489 \pm 0.897i$. The plant is unstable with

$$n_p = 4. \tag{67}$$

The zeros are approximately at $s \approx -1.1643 \pm 3.5712i, -5.8887 \pm 1.0513i$. The plant is minimum phase with

$$n_z = 4. \tag{68}$$

The number of asymptotes is

$$N_a = 2 \lfloor \frac{\sqrt{14} - \sqrt{7} + 1}{2} \rfloor = 2. \tag{69}$$

The asymptote angles are

$$\phi = \pm \frac{\pi}{\sqrt{14} - \sqrt{7}} \approx \pm 164.25°. \tag{70}$$

Thus, the number of branches is

$$N_b = 6. \tag{71}$$

Since $n_p = 4$, we immediately see that, for sufficiently large k, two additional poles must enter the LHP by crossing the branch cut. Moreover, because the locus has only LHP zeros and asymptotes, the two RHP poles must eventually migrate to the LHP. Thus, (66) can be stabilized by proportional control alone. Note that in this example, we do not calculate arrival/departure angles because they do not affect the stability conclusions being drawn. The root locus is shown in Fig. 4.

Were we to approximate each exponent to the first decimal and apply the mapping $s = \nu^{10}$, the ν-plane locus would contain 37 branches. However, on the slit s-plane, there are only 6 branches. This is because the closed-loop denominator has only positive coefficients, and thus, from Theorem 2.3, has at most $2\lfloor \sqrt{14} \rfloor = 6$ roots on the slit s-plane. This reduction in complexity is a clear advantage of constructing the locus directly on the slit s-plane.
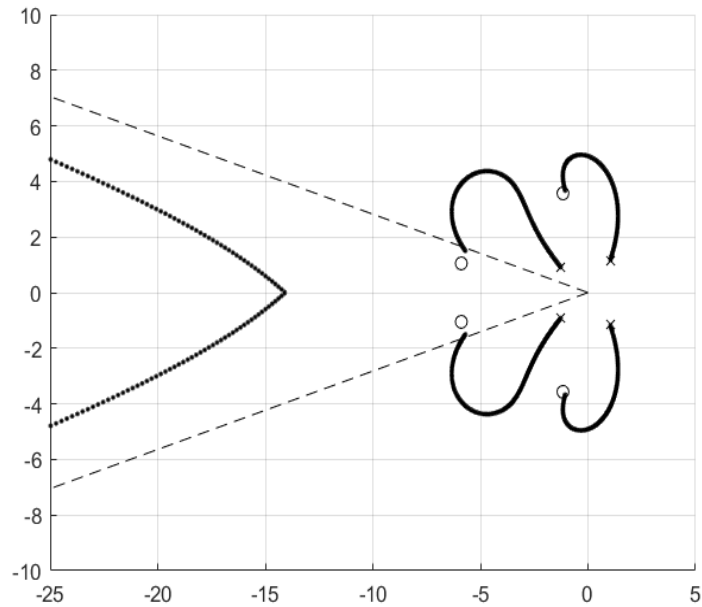
Figure 4: Fractional locus for (66).

2.4.2 Example

Consider the plant

$$P(s) = \frac{s-1}{s^{\sqrt{2}}(s+2)}. \tag{72}$$

The plant is neutrally stable. Noting the zero at $s = 1$, the plant is non-minimum phase with

$$n_z = 1. \tag{73}$$

The number of asymptotes is

$$N_a = 2\lfloor \frac{\sqrt{2}+1}{2} \rfloor = 2. \tag{74}$$

The asymptote angles are

$$\phi = \pm\frac{\pi}{\sqrt{2}} \approx 127.28° \tag{75}$$

Thus, the number of branches is

$$N_b = 3. \tag{76}$$

Because of the branch lying along the real-axis between the origin and RHP zero, proportional control cannot stabilize this system. The root locus is shown in Fig. 5.

18

Examining Fig. 2, we see that the controller, C_0,

$$C_0(s) = k\frac{s-2}{s+1}, \tag{77}$$

will stabilize P for sufficiently small k. Because of the controller RHP zero, the locus can no longer lie on the real-axis between the origin and the plant zero at $s = 1$. Furthermore, C_0 does not affect the asymptotic order of the loop gain, so the number of asymptotes remains unchanged. Consequently, the number of branches is now

$$N_b = 4. \tag{78}$$

The depature angles from $s = -2$ are

$$\psi = \pm(2 - \sqrt{2})\pi \approx \pm105.44°. \tag{79}$$

Thus, these two poles depart toward the LHP asymptotes. The departure angles from $s = -1$ are

$$\psi = \pm(3 - \sqrt{2})\pi \approx \pm285.44°. \tag{80}$$

Hence, these two poles immediately leave the slit s-plane. The departure angles from $s = 0$ are

$$\psi = \pm\frac{\pi}{\sqrt{2}} \approx \pm127.28°. \tag{81}$$

Therefore, these two poles depart in the LHP. Consequently, C_0 stabilizes P for sufficiently small k. The root locus is shown in Fig. 6. To determine the actual value of the stabilizing k, the loop gain can be analyzed with the Nyquist plot, shown in Fig. 7, which indicates that $k = 0.1$ is sufficiently small.
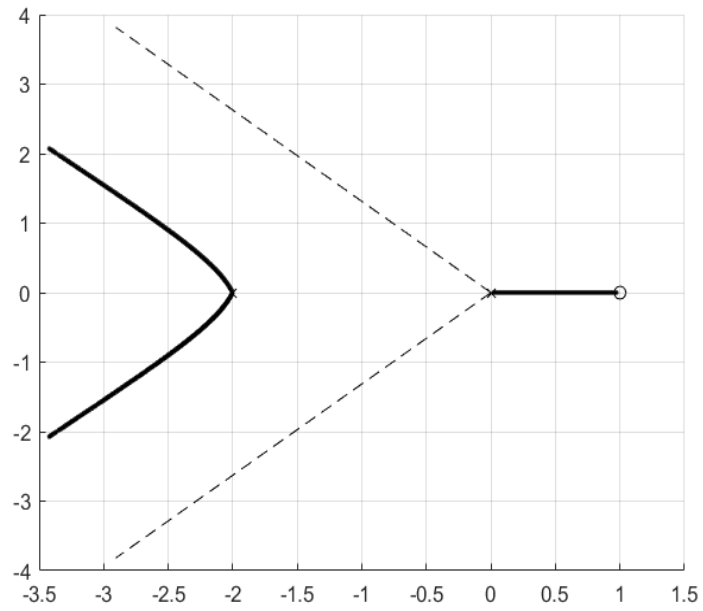
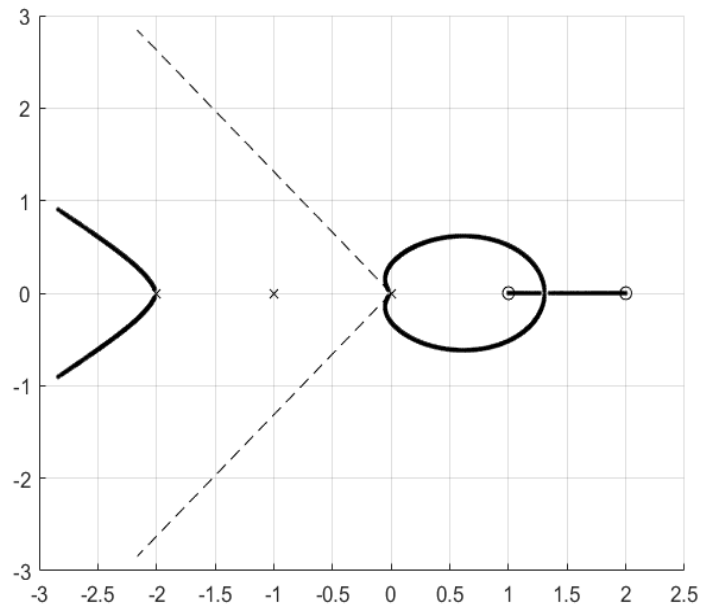Figure 5: Fractional locus for (72).

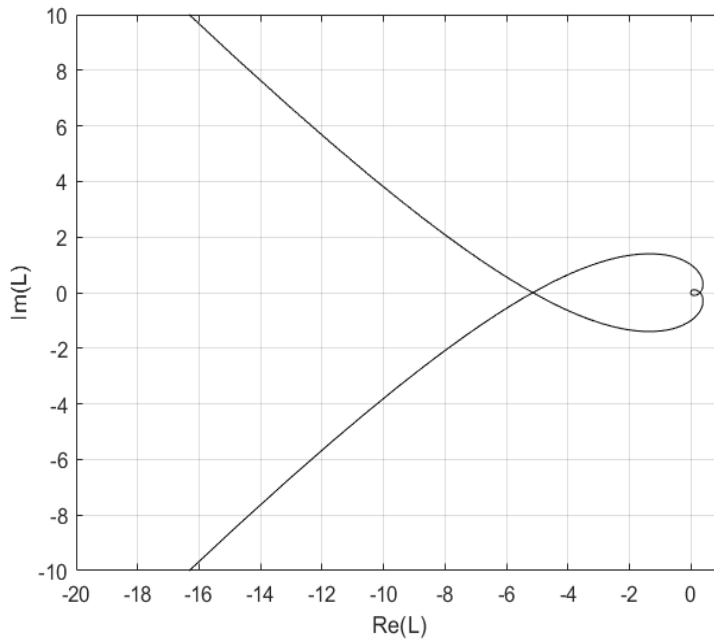Figure 6: Fractional locus using (77) to control (72).

20

Figure 7: Nyquist plot using (77) to control (72).

3 Fractional $\mathscr{H}_2$

The $\mathscr{H}_2$ problem is to design an output feedback controller that minimizes the square sum of weighted transfer functions of the closed-loop. Because these transfer functions represent all potential input-output relationships of the control system, this framework captures a wide variety of minimum energy problems in optimal control and filtering. Moreover, while not directly concerned with robustness as in the $\mathscr{H}_\infty$ problem, the optimal $\mathscr{H}_2$ controller often has desirable robustness properties in practice. Of course, it should also be emphasized that the Wiener-Hopf solution to the $\mathscr{H}_2$ problem is mechanistic and easy to understand. These features make the $\mathscr{H}_2$ problem a useful paradigm for analytical controller design.

3.1 Youla Parameterization

We consider the $\mathscr{H}_2$ problem for scalar, fractional plants, P, of minimizing

$$\min_C \sum ||W_i T_i||_2^2, \tag{82}$$

where the W_i are stable and minimum-phase weighting functions, and the T_i are the closed-loop transfer functions:

$$T_1 = \frac{P}{1 + PC}, \tag{83}$$

$$T_2 = \frac{PC}{1 + PC}, \tag{84}$$

$$T_3 = \frac{C}{1 + PC}, \tag{85}$$

$$T_4 = \frac{1}{1 + PC}. \tag{86}$$

Because the T_i are nonlinear in C, we seek a parameterization in which the T_i are affine to facilitate solution via Wiener-Hopf spectral factorization.

A seemingly reasonable approach used by [16], inherited from [13], is to parameterize all controllers, C, in terms of H,

$$C = \frac{P - H}{PH}. \tag{87}$$

This transforms the T_i into affine functions of H:

$$T_1 = H, \tag{88}$$

$$T_2 = \frac{P - H}{P}, \tag{89}$$

$$T_3 = \frac{P - H}{P2}, \tag{90}$$

$$T_4 = \frac{H}{P}. \tag{91}$$

Examining the T_i, one wonders if they are necessarily proper. Of course, for the $\mathcal{H}_2$ problem to be well-posed, any $W_i T_i$ appearing in the cost function must be proper, though from this it does not follow that each T_i is itself proper. As noted in [6, 7], nothing in the Wiener-Hopf procedure guarantees the properness of the T_i. Nevertheless, this is a minor issue as H may always be rolled-off *ex post facto* to recover properness of the T_i. The true problem with this parameterization scheme is that if P is non-minimum-phase, then $T_3 = P^{-1} - P^{-2}H$ is unstable. Even if T_3 does not describe an explicit input-output relationship of the system, it still describes an internal signal or hidden mode of the closed-loop. Since the closed-loop must not contain unstable hidden modes, we require that the parameterization ensure the stability of each T_i regardless

of whether or not they appear in the cost function, that is to say, we require that the parameterization preserve *internal stability*.

Internal stability is intimately connected to observability and controllability. Typically, fractional order observability and controllability are discussed in the time-domain, and as such, rest on a tenuous notion of pseudo state-spaces, defined only for commensurate order systems [10]. While fractional systems do not have well-defined states, they possess a finite number of ordinary poles and zeros (see Theorem 2.3). It is through this feature that fractional systems bear the strongest resemblance to rational systems. Hence, a more useful definition of fractional order observability and controllability can be found by tracing the concept of unstable hidden modes to the infamous RHP pole-zero cancellations between P and C. To illustrate, suppose P is non-minimum phase. If C is parameterized in terms of H, then the term, PH, appears in the denominator of C. Since H must be stable, no pole of H can cancel a non-minimum-phase zero of P. In other words, the RHP zeros of P are preserved as RHP poles of C. Consequently, when P and C are in series, the unstable controller poles are necessarily cancelled by non-minimum phase plant zeros. This cancellation renders those controller modes unobservable, the effect of which is the instability of the internal signal, $T_3 = C(1 + PC)^{-1}$. Therefore, a parameterization satisfying internal stability is one that forbids RHP pole-zero cancellations between P and C. Indeed, this was the original motivation behind the Youla parameterization for rational plants [18], which has since been generalized to fractional plants [2, 12].

The fractional order Youla parameterization can be constructed as follows. Let $\mathscr{F}_\infty$ denote the set of fractional order, stable, and proper transfer functions. We factor P into the ratio of two transfer functions,

$$P = \frac{B}{A}, \tag{92}$$

where $A, B \in \mathscr{F}_\infty$. Suppose we find a nominal stabilizing controller, C_0, which we similarly factor into

$$C_0 = \frac{Y_0}{X_0}, \tag{93}$$

where $X_0, Y_0 \in \mathscr{F}_\infty$. We construct these factors to satisfy

$$AX_0 + BY_0 = F, \tag{94}$$

where $F, F^{-1} \in \mathscr{F}_\infty$. We then define

$$X = \frac{X_0}{F}, \tag{95}$$

23

$$Y = \frac{Y_0}{F}, \tag{96}$$

where $X, Y \in \mathscr{F}_\infty$. Consequently, A, B, X, Y satisfy Bezout's identity,

$$AX + BY = 1. \tag{97}$$

We then parameterize all controllers, C, in terms of Q,

$$C = \frac{Y - AQ}{X + BQ}. \tag{98}$$

Using (92), (97), and (98), the T_i are affine in Q:

$$T_1 = B(X + BQ), \tag{99}$$

$$T_2 = B(Y - AQ), \tag{100}$$

$$T_3 = A(Y - AQ), \tag{101}$$

$$T_4 = A(X + BQ). \tag{102}$$

If Q is stable and proper, then the T_i are stable and proper. Thus, the $\mathscr{H}_2$ problem becomes

$$\min_Q \sum ||W_i T_i||_2^2, \tag{103}$$

subject to the constraint that Q is stable and proper. Note that if P is rational, then Bezout's identity can be solved algebraically without knowledge of C_0 to generate the factors X, Y [6]. However, if P is fractional, then knowledge of C_0 is required to generate the factors X, Y. Thus, classical control techniques are especially important for fractional systems because of the need to know this nominal stabilizing controller.

Given the Youla parameterization, the cost function is quadratic in Q. We are now in a position to use Wiener-Hopf spectral factorization. The optimal Q satisfies

$$\Omega^- = \frac{\partial}{\partial \bar{Q}} \sum |W_i T_i|^2, \tag{104}$$

where Ω^- is analytic in the LHP [4]. Because the sum is over the square modulus of affine functions of Q,

$$\Omega^- = M + VQ, \tag{105}$$

where M and V are mixed functions possessing singularities in both the RHP and LHP. In terms of the weightings W_i, and factors, A, B, X, Y,

$$M = |W_1 B|^2 \bar{B} X - |W_2 B|^2 \bar{A} Y - |W_3 A|^2 \bar{A} Y + |W_4 A|^2 \bar{B} X, \tag{106}$$

$$V = |W_1 B^2|^2 + |W_2 BA|^2 + |W_3 A^2|^2 + |W_4 AB|^2. \tag{107}$$

Suppose we know the product decomposition, $V = V^+ V^-$, such that V^+, V^-, and their reciprocals are analytic in the RHP and LHP, respectively. Further suppose we know the additive decomposition, $M/V^- = \{M/V^-\}_+ + \{M/V^-\}_-$, where $\{M/V^-\}_+$ and $\{M/V^-\}_-$ are analytic in the RHP and LHP, respectively. Given these decompositions,

$$\frac{\Omega^-}{V^-} - \left\{ \frac{M}{V^-} \right\}_- = \left\{ \frac{M}{V^-} \right\}_+ + V^+ Q. \tag{108}$$

Since the LHS is purely unstable and the RHS is purely stable, equality holds if and only if both sides are null. We may therefore argue from analytic continuity [11, 13] that the optimal stable Q is

$$Q = -\frac{1}{V^+} \left\{ \frac{M}{V^-} \right\}_+. \tag{109}$$

Note that just as in the case of a rational plant, the Wiener-Hopf procedure does not necessarily result in a proper Q. If the resulting Q is improper, then it is necessary to roll it off after a specified cut-off frequency, ω_c,

$$Q \rightarrow Q \left(\frac{\omega_c}{s + \omega_c} \right)^\nu, \tag{110}$$

where ν is chosen so that Q becomes proper. Thus, (103) is satisfied in a limiting sense as $\omega_c \rightarrow \infty$ [7].

Beginning with the product decomposition, $V = V^+ V^-$, we immediately encounter a problem. When the weightings, W_i, and factors, A, B, X, Y, are rational transfer functions, V is the square modulus sum of rational transfer functions. In other words, V is itself a rational function and can be decomposed by factoring polynomials. However, when the W_i and A, B, X, Y are fractional transfer functions, V is the square modulus sum of fractional transfer functions and is not factorable through elementary methods. In particular, the numerator of V cannot be decomposed by factoring polynomials. Expressing V as

$$V = \frac{\gamma}{\chi}, \tag{111}$$

25

we see that because the W_i and A, B, X, Y are stable, χ has the form,

$$\chi = |f|^2, \tag{112}$$

where f is a stable fractional polynomial. Thus, the factorization, $\chi = \chi^+ \chi^-$, is trivial:

$$\chi^+ = f, \tag{113}$$

$$\chi^+ = \bar{f}. \tag{114}$$

On the other hand, γ has the form,

$$\gamma = \sum |f_i|^2, \tag{115}$$

where each f_i is a fractional polynomial. One might think that if the f_i are commensurate order, that the factorization of γ should reduce to a polynomial factorization under the transformation, $s = \nu^r$. However, even if $f_i = f_i(s)$ is a single-valued polynomial in $s = \nu^r$, $\bar{f}_i = f_i(-s)$ is not a single-valued polynomial in $s = \nu^r$, but rather, $s = -\nu^r$. Thus, there does not exist a mapping plane where γ becomes a single-valued polynomial. In other words, γ is not factorable through elementary methods even if each f_i is commensurate order. Consequently, we factor γ using an integral factorization technique.

3.2 Integral Factorization Technique

In the context of diffraction theory and partial differential equations, Noble discusses the product decomposition of kernels with branch point singularities in great detail [11]. The key idea is to use the logarithm to transform the product decomposition into the additive decomposition, for which there is a well-known constructive formula [11], [13], [16]. We begin with a review of the integral factorization technique in [11].

Suppose we want the additive decomposition, $\Phi = \Phi_+ + \Phi_-$. Assuming that $\Phi(t) = \mathscr{L}^{-1}[\Phi(s)]$ exists, Φ can be additively decomposed into its causal and anti-causal parts in the time-domain,

$$\Phi(t) = \theta(t)\Phi(t) + (1 - \theta(t))\Phi(t), \tag{116}$$

where $\theta(t)$ is the Heaviside step function i.e. $\theta(t) = 1$ for $t \geq 0$ and $\theta(t) = 0$ otherwise. Transforming back to the the frequency domain,

$$\Phi(s) = \mathscr{L}\{\theta(t)\Phi(t)\} + \mathscr{L}\{(1 - \theta(t))\Phi(t)\}. \tag{117}$$

We can associate Φ_+ and Φ_- with the first and second term in the sum, respectively:

$$\Phi_+(s) = \mathscr{L}\{\theta(t)\mathscr{L}^{-1}[\Phi(s)]\}, \tag{118}$$

$$\Phi_-(s) = \mathscr{L}\{(1 - \theta(t))\mathscr{L}^{-1}[\Phi(s)]\}. \tag{119}$$

Now suppose we want the product decomposition, $\Psi = \Psi^+\Psi^-$. We can simply define

$$\Phi = \log\Psi. \tag{120}$$

Again assuming that $\Phi(t) = \mathscr{L}^{-1}[\Phi(s)]$ exists, the additive decomposition, $\Phi = \Phi_+ + \Phi_-$, can be obtained, resulting in

$$\log\Psi = \Phi_+ + \Phi_-. \tag{121}$$

After exponentiating,

$$\Psi = \exp(\Phi_+ + \Phi_-) = \exp\Phi_+ \exp\Phi_-, \tag{122}$$

we can associate Ψ^+, Ψ^- with the first and second term in the product, respectively:

$$\Psi^+(s) = \exp(\mathscr{L}\{\theta(t)\mathscr{L}^{-1}[\log\Psi(s)]\}), \tag{123}$$

$$\Psi^+(s) = \exp(\mathscr{L}\{(1 - \theta(t))\mathscr{L}^{-1}[\log\Psi(s)]\}). \tag{124}$$

In light of this integral factorization technique, one might be tempted to directly inverse transform $\log\gamma$ or perhaps $\log(1/\gamma)$. However, as $|s| \to \infty$, both $\log\gamma$ and $\log(1/\gamma)$ diverge. Thus, we define

$$\Phi = \log\frac{\gamma}{\lambda}, \tag{125}$$

where λ is an appropriate reference function. At the very least, λ must have the same leading order as γ to ensure that at high-frequency, $\gamma/\lambda \to 1$, so that $\Phi = \log(\gamma/\lambda) \to 0$. This alone, however, does not guarantee that $\Phi(t) = \mathscr{L}^{-1}[\Phi(s)]$ exists. In particular, if $\Phi(s)$ decays too slowly at high-frequency, then $\Phi(t)$ near $t = 0$ becomes unbounded, making time domain additive decomposition numerically fraught. This can be seen from the initial value theorem for the inverse bilateral Laplace transform [5]:

$$\lim_{s\to\infty} s\Phi = \mathscr{L}^{-1}(\Phi(s))|_{t=0^+} - \mathscr{L}^{-1}(\Phi(s))|_{t=0^-}. \tag{126}$$

The terms on the RHS are the values of $\Phi(t)$ near $t = 0$. Since these need to be computable, we require that as $|s| \to \infty$,

$$\mathscr{O}(\Phi) \leq \mathscr{O}(s^{-1}), \tag{127}$$

where $\mathscr{O}(\Phi)$ denotes the asymptotic growth rate of $\Phi(s)$ as $|s| \to \infty$. In other words, we must choose a λ that has a similar enough growth rate to γ, such that Φ decays superlinearly. Given this condition,

$$\frac{\gamma}{\lambda} = \exp \Phi_+ \exp \Phi_-. \tag{128}$$

Now we see that in order for λ to be useful, the factorization, $\lambda = \lambda^+ \lambda^-$, must be known. Given this factorization,

$$\gamma^+ = \lambda^+ \exp \Phi_+, \tag{129}$$

$$\gamma^- = \lambda^- \exp \Phi_-. \tag{130}$$

This is a constructive formula for the factorization of γ.

To obtain a suitable λ, we assume that for some n,

$$\mathscr{O}(|f_n|^2) \geq \mathscr{O}(s \sum_{i \neq n} |f_i|^2). \tag{131}$$

The simplest choice of λ appears to be

$$\lambda = |f_n|^2. \tag{132}$$

Examining $\Phi = \log \gamma / \lambda$,

$$\Phi = \log \frac{|f_n|^2 + \sum_{i \neq n} |f_i|^2}{|f_n|^2}. \tag{133}$$

Noting that for small x, $\log(1 + x) \to x$,

$$\Phi \to \frac{\sum_{i \neq n} |f_i|^2}{|f_n|^2}. \tag{134}$$

Hence, $\mathscr{O}(\Phi) \leq \mathscr{O}(s^{-1})$.

Now we simply need to factor $\lambda = |f_n|^2$. If f_n is stable, then this factorization is trivial: $\lambda^+ = f_n$ and $\lambda^- = \bar{f}_n$. However, if f_n is unstable, then we need to factor both the roots and branch points of $|f_n|^2$. Though the number of roots of a fractional polynomial on the primary Riemann sheet can be arbitrarily large, the number of roots is still finite (see Theorem 2.3). Thus, for a given f_n, there are only a finite

number of roots with finite multiplicity. Hence, we can define z, the polynomial formed by the product of the RHP roots of f_n. We can use z to extract the stable part of f_n, μ,

$$\mu = \frac{f_n}{z}. \tag{135}$$

The function, μ, is well defined at the roots of z because these are removable singularities of μ [3]. Thus, μ has neither poles nor zeros at any of the original roots of f_n, implying that its only singularities are the leftover branch points of f_n, which are stable. Consequently, the factorization of λ is simply

$$\lambda^+ = [f_n \bar{f}_n]^+ = [\mu z \bar{\mu} \bar{z}]^+ = \mu \bar{z}, \tag{136}$$

$$\lambda^- = [f_n \bar{f}_n]^- = [\mu z \bar{\mu} \bar{z}]^- = \bar{\mu} z. \tag{137}$$

If f_n is commensurate order, then it is possible to obtain z analytically, in which case μ will also algebraically reduce i.e. the poles will be explicitly canceled as in the method of [16]. The algebraic reduction of μ, however, is immaterial to whether or not the factorization of λ is valid as a theoretical construct, and thus, applies equally to incommensurate order f_n. Therefore, the factorization, $\gamma = \gamma^+ \gamma^-$, can always be obtained in principle from (129), (130), (136), (137).

Nevertheless, choosing $\lambda = |f_n|^2$ is impractical. If f_n is incommensurate order, then z must be obtained numerically. Because of imperfect knowledge of z, there will be an imperfect cancellation between f_n and z, so μ will technically have an unstable pole with a small residue. Even if f_n is commensurate order, calculation of z in the mapping plane can be cumbersome if the fractional exponents have high precision. Thus, we provide a method to factor γ that does not require root calculation.

Theorem 3.1. *Consider $\gamma = \sum |f_i|^2$. There exist fractional polynomials g, h, such that $f_n = g + h$, g is stable, and $\mathcal{O}(g) \geq \mathcal{O}(sh)$. Choosing $\lambda = |g|^2$, we can additively decompose $\Phi = \log \gamma / \lambda$, which implies*

$$\gamma^+ = g \exp \Phi_+, \tag{138}$$

$$\gamma^- = \bar{g} \exp \Phi_-. \tag{139}$$

Proof. We express f_n as

$$f_n = p + q, \tag{140}$$

29

where $\mathcal{O}(p) \geq \mathcal{O}(sq)$. Consider a stable fractional polynomial, r, satisfying

$$\mathcal{O}(s^2 r) > \mathcal{O}(p) \geq \mathcal{O}(sr). \tag{141}$$

We can construct the fractional polynomial, $p + kr$, where k is a positive constant. The roots of $p + kr$ are points on the root locus of

$$1 + k\frac{r}{p} = 0. \tag{142}$$

The asymptotes angles (39) are

$$\phi = \pm\frac{\pi}{\delta} \tag{143}$$

where $\delta \in [1, 2)$. Thus, the asymptotes of the locus are in the LHP. Because r is stable, the zeros of the locus are also in the LHP. Therefore, there exists a finite, positive k such that all poles of the locus, or roots of $p + kr$, are in the LHP. In other words, $p + kr$ is stable.

Now, we can express f_n as

$$f_n = g + h \tag{144}$$

where

$$g = p + kr, \tag{145}$$

$$h = -kr + q. \tag{146}$$

By construction, g is stable and $\mathcal{O}(g) \geq \mathcal{O}(sh)$.

Choosing $\lambda = |g|^2$, $\Phi = \log\gamma/\lambda$ becomes

$$\Phi = \log\frac{|g|^2 + g\bar{h} + \bar{g}h + |h|^2 + \sum_{i\neq n}|f_i|^2}{|g|^2}. \tag{147}$$

Noting that for small x, $\log(1 + x) \to x$,

$$\Phi \to \frac{g\bar{h} + \bar{g}h + |h|^2 + \sum_{i\neq n}|f_i|^2}{|g|^2}. \tag{148}$$

Thus, $\mathcal{O}(\Phi) \leq \mathcal{O}(s^{-1})$. Since $\lambda^+ = g$ and $\lambda^- = \bar{g}$, (129) and (130) reduce to (138) and (139). $\qquad\square$

An important step in Theorem 3.1 is constructing a stable $g = p + kr$, where $\mathcal{O}(p) \geq \mathcal{O}(sr)$. While the locus can be used to accomplish this, Corollary 3.1.1 commonly yields a simpler way to construct g. Likewise, if f_n can be expressed as the product of fractional polynomials, then Corollary 3.1.2 is helpful when constructing g.

Corollary 3.1.1. *Consider $f_n = p + q$, where p contains the leading term and all other terms within one order of the leading term (e.g. if $f_n(s) = 8s^{\sqrt{8}} + 6s^{\sqrt{6}} + 5s^{\sqrt{5}} + 3s^{\sqrt{3}} + 2s^{\sqrt{2}} - 1$, then $p(s) = 8s^{\sqrt{8}} + 6s^{\sqrt{6}} + 5s^{\sqrt{5}}$ and $q(s) = 3s^{\sqrt{3}} + 2s^{\sqrt{2}} - 1$). Assume each term in p has positive coefficients. We denote the smallest exponent in p as $m\delta$, where $\delta \in [1, 2)$ and m is a positive integer. If we choose g as,*

$$g(s) = \frac{(s^\delta + 1)^m p(s)}{s^{m\delta}}, \tag{149}$$

then $f_n = g + h$, where g is stable and $\mathscr{O}(g) \geq \mathscr{O}(sh)$.

Proof. By construction, $\mathscr{O}(p(s)/s^{m\delta}) \leq \mathscr{O}(s)$. By assumption, the coefficients of p are positive. Hence, from Theorem 2.1, $p(s)/s^{m\delta}$ is stable. Thus, g is stable. Expanding g,

$$g(s) = \frac{(s^{m\delta} + ms^{(m-1)\delta} + ...)p(s)}{s^{m\delta}}, \tag{150}$$

$$g(s) = (1 + ms^{-\delta} + ...)p(s). \tag{151}$$

If we define $r(s) = (ms^{-\delta} + ...)p(s)$, then $g = p + r$, where $\mathscr{O}(g) \geq \mathscr{O}(sr)$. By construction, $\mathscr{O}(p) \geq \mathscr{O}(sq)$. Therefore, $\mathscr{O}(g) \geq \mathscr{O}(sh)$, where $h = -r + q$. □

Corollary 3.1.2. *Consider $f_n = \prod p_j$, where each p_j is a fractional polynomial. If each $p_j = g_j + h_j$, where g_j is stable and $\mathscr{O}(g_j) \geq \mathscr{O}(sh_j)$, then $f_n = g + h$, where g is stable and $\mathscr{O}(g) \geq \mathscr{O}(sh)$.*

Proof. Expanding $f_n = \prod p_j = g + h$,

$$g = \prod g_j, \tag{152}$$

$$\mathscr{O}(h) = \mathscr{O}(\prod_{j \neq m} g_j h_m). \tag{153}$$

If each g_j is stable, then g is stable. If each g_j satisfies $\mathscr{O}(g_j) \geq \mathscr{O}(sh_j)$, then $\mathscr{O}(g) \geq \mathscr{O}(sh)$. □

Given the factorization, $\gamma = \gamma^+ \gamma^-$, the product decomposition, $V = V^+ V^-$, is

$$V^+ = \frac{\gamma^+}{\chi^+}, \tag{154}$$

$$V^- = \frac{\gamma^-}{\chi^-}. \tag{155}$$

where V is given by (107). The stable term in the additive decomposition, $M/V^- = \{M/V^-\}_+ + \{M/V^-\}_-$, is

$$\left\{ \frac{M}{V^-} \right\}_+ = \mathscr{L}\left[\theta(t) \mathscr{L}^{-1}\left(\frac{M}{V^-} \right) \right], \tag{156}$$

31

where M is given by (106). Therefore, the optimal Q (109) is solved. Once Q is known, the optimal controller, C (98), is completely specified. Note that while Q is infinite dimensional, the integrals that define Q can be computed efficiently and arbitrarily accurately over a specified bandwidth, for instance, with the standard fast Fourier transform and inverse fast Fourier transform algorithms [10].

For implementation, the infinite-dimensional C can be approximated with a rational function. Of course, it is possible to approximate the plant from the outset and then subsequently design a controller based on the approximation. However, in so doing, the approximation error in the plant is indirectly transmitted to the controller. Undoubtedly, there are cases where approximating the plant yields satisfactory results. Yet, this misses the point that even in cases where a plant approximation suffices, the ability to directly construct the infinite-dimensional controller enables one to gauge the validity of that plant approximation. In other words, an implicit description of C is valuable even if the integral formalism is not used to implement it. That is not to say that an implicit description of C should only be used for verification purposes. In fact, direct construction of C and subsequently approximating it with a rational function is straightforward and effective, which we demonstrate by example in the next section.

3.3 Examples

In the following examples, we use spectral factorization to construct the optimal $\mathscr{H}_2$ output feedback controller for both a non-mimum phase neutrally stable plant and a minimum phase unstable plant.

3.3.1 Example

Consider the non-minimum phase, neutrally stable plant and nominal stabilizing controller in Example 2.4.2,

$$P(s) = \frac{s-1}{s^{\sqrt{2}}(s+2)}, \qquad C_0(s) = \frac{0.1(s-2)}{s+1}. \tag{157}$$

Suppose we choose constant weightings, $W_1 = 1, W_2 = 2, W_3 = 0, W_4 = 0$.

To construct the fractional order Youla parameterization, we factor the plant as $P = BA^{-1}$,

$$B(s) = \frac{s-1}{(s^{\sqrt{2}}+1)(s+2)}, \tag{158}$$

$$A(s) = \frac{s^{\sqrt{2}}}{s^{\sqrt{2}}+1}, \tag{159}$$

32

where $A, B \in \mathscr{F}_\infty$. We factor the nominal stabilizing controller as $C_0 = Y_0 X_0^{-1}$,

$$Y_0(s) = \frac{0.1(s-2)}{s+1}, \tag{160}$$

$$X_0 = 1, \tag{161}$$

where $X_0, Y_0 \in \mathscr{F}_\infty$. Observe that $AX_0 + BY_0 = F$,

$$F(s) = \frac{s^{\sqrt{2}}(s+2)(s+1) + 0.1(s-1)(s-2)}{(s^{\sqrt{2}}+1)(s+2)(s+1)}, \tag{162}$$

where $F, F^{-1} \in \mathscr{F}_\infty$. Thus, $X = X_0 F^{-1}, Y = Y_0 F^{-1} \in \mathscr{F}_\infty$.

We require the product decomposition, $V = V^+ V^-$, where from (107),

$$V(s) = \frac{\gamma(s)}{\chi(s)} = \frac{|f_2(s)|^2 + |f_1(s)|^2}{|((s^{\sqrt{2}}+1)(s+2))^2|^2}, \tag{163}$$

$$f_2(s) = 2s^{\sqrt{2}}(s+2)(s-1), \tag{164}$$

$$f_1(s) = (s-1)^2. \tag{165}$$

The factorization, $\chi = \chi^+ \chi^-$, can be performed by inspection:

$$\chi^+(s) = ((s^{\sqrt{2}}+1)(s+2))^2, \tag{166}$$

$$\chi^-(-s) = (((-s)^{\sqrt{2}}+1)(-s+2))^2. \tag{167}$$

The unstable fractional polynomials comprising f_2 can be expressed as $g_j + h_j$, where g_j is stable and $\mathscr{O}(g_j) \geq \mathscr{O}(sh_j)$:

$$s^{\sqrt{2}} = (s^{\sqrt{2}}+1) - 1, \tag{168}$$

$$s - 1 = (s+1) - 2. \tag{169}$$

Hence, $f_2 = g + h$,

$$g(s) = 2(s^{\sqrt{2}}+1)(s+2)(s+1), \tag{170}$$

$$\mathscr{O}(h) = \mathscr{O}(s^{\sqrt{2}+1}), \tag{171}$$

where g is stable and $\mathscr{O}(g) \geq \mathscr{O}(sh)$. Thus, the product decomposition, $\gamma = \gamma^+ \gamma^-$, is given by Theorem 3.1.

From γ^+, γ^- and χ^+, χ^-, we construct V^+, V^-. From A, B, X, Y, we determine M (106), and compute the additive decomposition, $\{M/V^-\} = \{M/V^-\}_+ + \{M/V^-\}_-$. From V^+ and $\{M/V^-\}_+$, we compute Q

(109). Since Q is improper, we roll it off choosing $\omega_c = 100$ in (110), as shown in Fig. 8. From A, B, X, Y and Q, we construct C (98). For implementation, we use the `tfest` command in MATLAB [9] to approximate the rolled-off C with the rational $\tilde{C}$,

$$\tilde{C} = \frac{-3.7719(s + 76.21)(s + 25.82)(s + 7.282)(s + 1.646)(s + 0.2807)}{(s + 96.65)(s + 41.66)(s + 12.58)(s + 3.187)(s + 0.5704)}. \tag{172}$$

The Bode plots of the improper C and the approximate rolled-off $\tilde{C}$ are shown in Fig. 9. The magnitude plots of the resulting T_i are shown in Fig. 10. The closed-loop $y(t)$ and $u(t)$ are shown in Fig. 11.
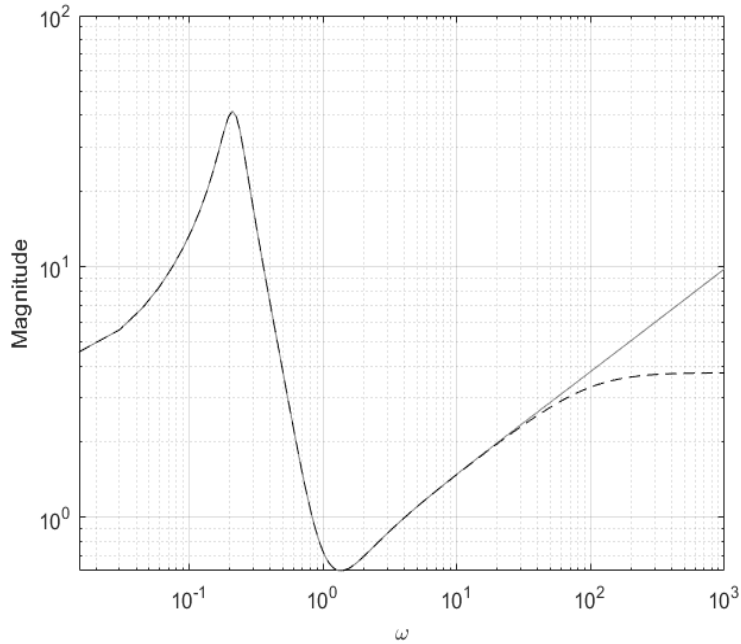
Figure 8: Example 3.3.1: optimal Q (gray), rolled-off Q (dashed).

3.3.2 Example

Consider the plant,

$$P(s) = \frac{s^{\sqrt{3}} + 1}{s^{\sqrt{13}} + s^3 - s^{\sqrt{7}} + 1}. \tag{173}$$

Though the plant is minimum-phase, it is unstable, which can be seen from Fig. 12. Because the locus has only LHP zeros and asymptotes, P can be stabilized by proportional control alone. A nominal stabilizing controller is
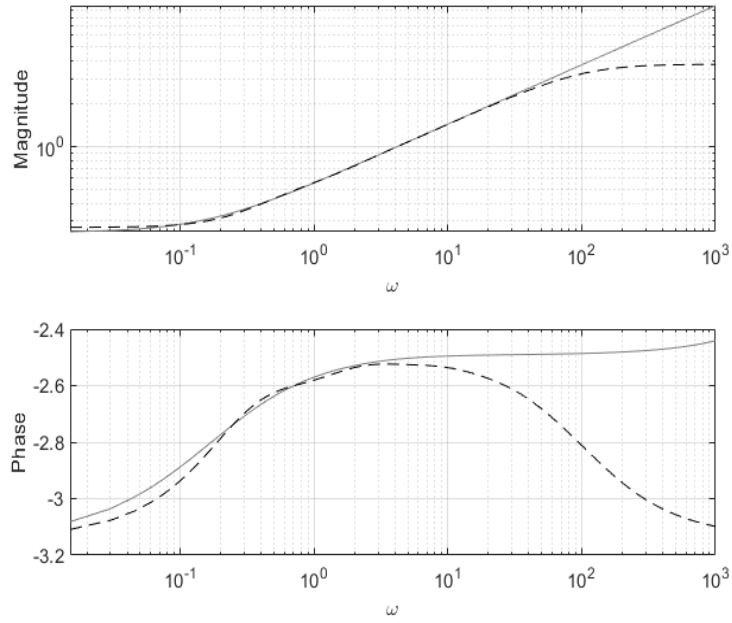
$$C_0 = 10, \tag{174}$$

34

Figure 9: Example 3.3.1: optimal controller, C (gray), approximate rolled-off controller, $\tilde{C}$ (dashed).
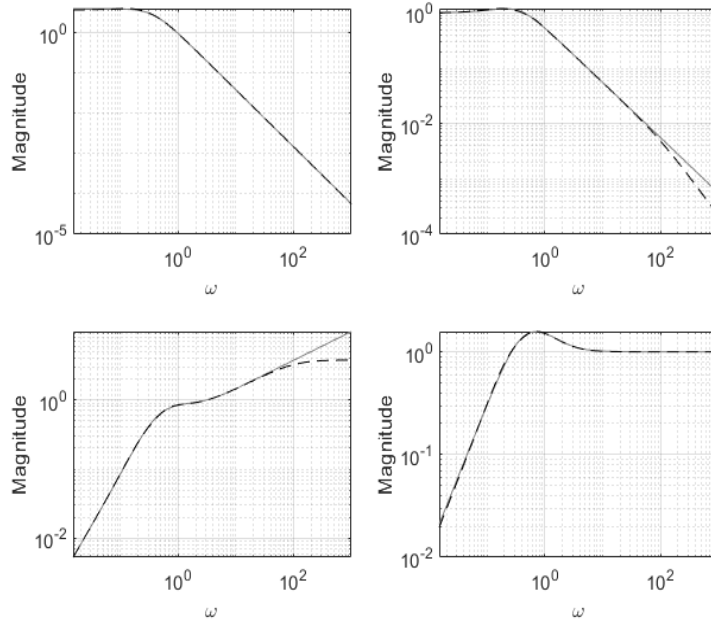

Figure 10: Example 3.3.1: optimal transfer functions, T_1 (upper left), T_2 (upper right), T_3 (bottom left), T_4 (bottom right), using C (gray), $\tilde{C}$ (dashed).
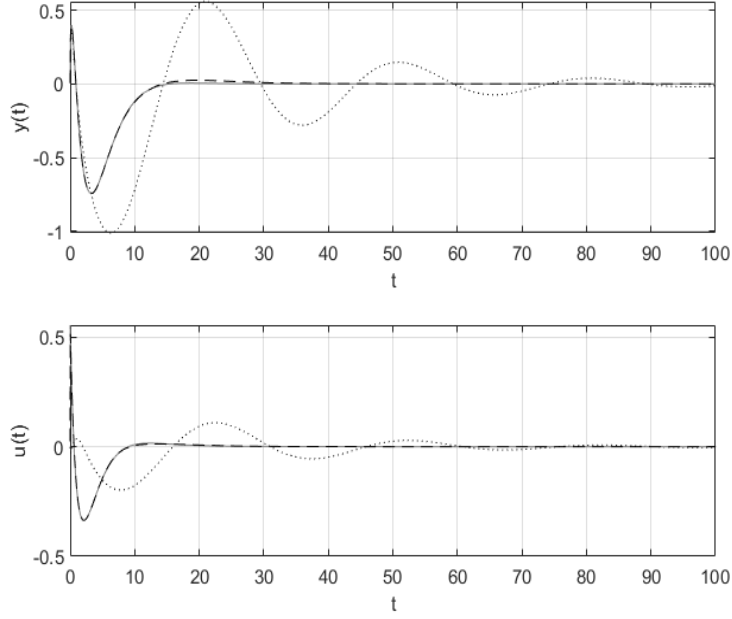
Figure 11: Example 3.3.1: optimal output, $y(t)$ (top), $u(t)$ (bottom), using C_0 (dotted), C (gray), $\tilde{C}$ (dashed).

which can be seen from Fig. 13. Suppose we choose constant weightings, $W_1 = 1, W_2 = 0.5, W_3 = 0, W_4 = 0$.

To construct the fractional order Youla parameterization, we factor the plant as $P = BA^{-1}$,

$$B(s) = \frac{s^{\sqrt{3}} + 1}{(s^{\sqrt{13}/3} + 1)^3}, \tag{175}$$

$$A(s) = \frac{s^{\sqrt{13}} + s^3 - s^{\sqrt{7}} + 1}{(s^{\sqrt{13}/3} + 1)^3}, \tag{176}$$

where $A, B \in \mathscr{F}_\infty$. We factor the nominal controller as $C_0 = Y_0 X_0^{-1}$,

$$Y_0 = 10, \tag{177}$$

$$X_0 = 1, \tag{178}$$

where $X_0, Y_0 \in \mathscr{F}_\infty$. Observe that $AX_0 + BY_0 = F$,

$$F(s) = \frac{s^{\sqrt{13}} + s^3 - s^{\sqrt{7}} + 10s^{\sqrt{3}} + 11}{(s^{\sqrt{13}/3} + 1)^3}, \tag{179}$$

where $F, F^{-1} \in \mathscr{F}_\infty$. Thus, $X = X_0 F^{-1}, Y = Y_0 F^{-1} \in \mathscr{F}_\infty$.

We require the product decomposition, $V = V^+ V^-$, where from (107),

$$V(s) = \frac{\gamma(s)}{\chi(s)} = \frac{|f_2(s)|^2 + |f_1(s)|^2}{|(s^{\sqrt{13}/3} + 1)^6|^2}, \tag{180}$$

36

$$f_2(s) = 0.5(s^{\sqrt{13}} + s^3 - s^{\sqrt{7}} + 1)(s^{\sqrt{3}} + 1), \tag{181}$$

$$f_1(s) = (s^{\sqrt{3}} + 1)^2. \tag{182}$$

The denominator factorization, $\chi = \chi^+ \chi^-$, can be performed by inspection:

$$\chi^+(s) = (s^{\sqrt{13}/3} + 1)^6, \tag{183}$$

$$\chi^-(-s) = ((-s)^{\sqrt{13}/3} + 1)^6. \tag{184}$$

The unstable fractional polynomial comprising f_2 can be expressed as $g_j + h_j$, where g_j is stable and $\mathscr{O}(g_j) \geq \mathscr{O}(sh_j)$:

$$s^{\sqrt{13}} + s^3 - s^{\sqrt{7}} + 1 = (s^{\sqrt{13}} + s^3 - s^{\sqrt{7}} + 10s^{\sqrt{3}} + 11) - 10(s^{\sqrt{3}} + 1). \tag{185}$$

Hence, $f_2 = g + h$,

$$g(s) = 0.5(s^{\sqrt{13}} + s^3 - s^{\sqrt{7}} + 10s^{\sqrt{3}} + 11)(s^{\sqrt{3}} + 1), \tag{186}$$

$$\mathscr{O}(h) = \mathscr{O}(s^{2\sqrt{3}}), \tag{187}$$

where g is stable and $\mathscr{O}(g) \geq \mathscr{O}(sh)$. Thus, the product decomposition, $\gamma = \gamma^+ \gamma^-$, is given by Theorem 3.1.

From γ^+, γ^- and χ^+, χ^-, we construct V^+, V^-. From A, B, X, Y, we determine M (106), and compute the additive decomposition, $\{M/V^-\} = \{M/V^-\}_+ + \{M/V^-\}_-$. From V^+ and $\{M/V^-\}_+$, we compute Q (109). Since Q is improper, we roll it off choosing $\omega_c = 100$ in (110), as shown in Fig. 14. From A, B, X, Y and Q, we construct C (98). For implementation, we use the `tfest` command in MATLAB [9] to approximate the rolled-off C with the rational $\tilde{C}$,

$$\tilde{C} = \frac{168.97(s + 43.32)(s + 11.11)(s + 1.965)(s^2 + 0.5236s + 0.2289)}{(s + 94.36)(s + 35.59)(s + 8.017)(s^2 + 0.5204s + 0.9828)} \tag{188}$$

The Bode plots of the improper C and the approximate rolled-off $\tilde{C}$ are shown in Fig. 15. The magnitude plots of the resulting T_i are shown in Fig. 16. The closed-loop $y(t)$ and $u(t)$ are shown in Fig. 17.
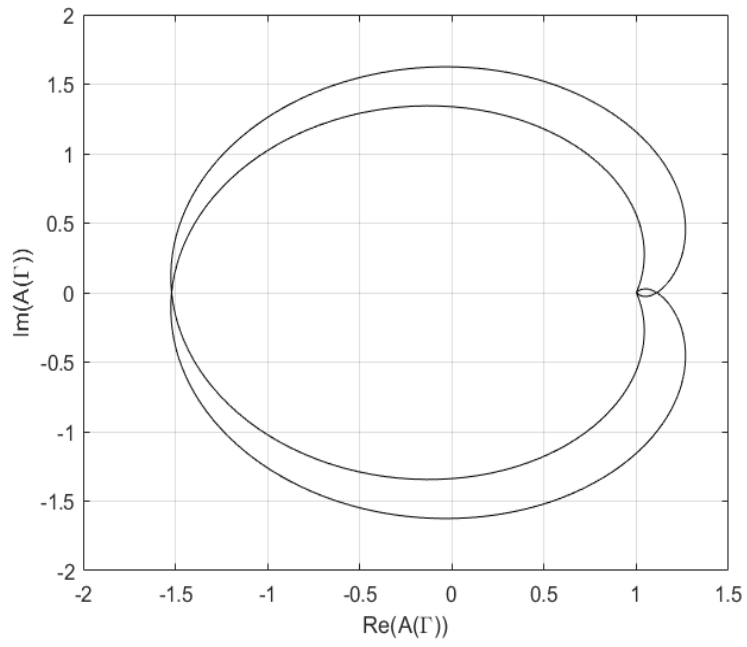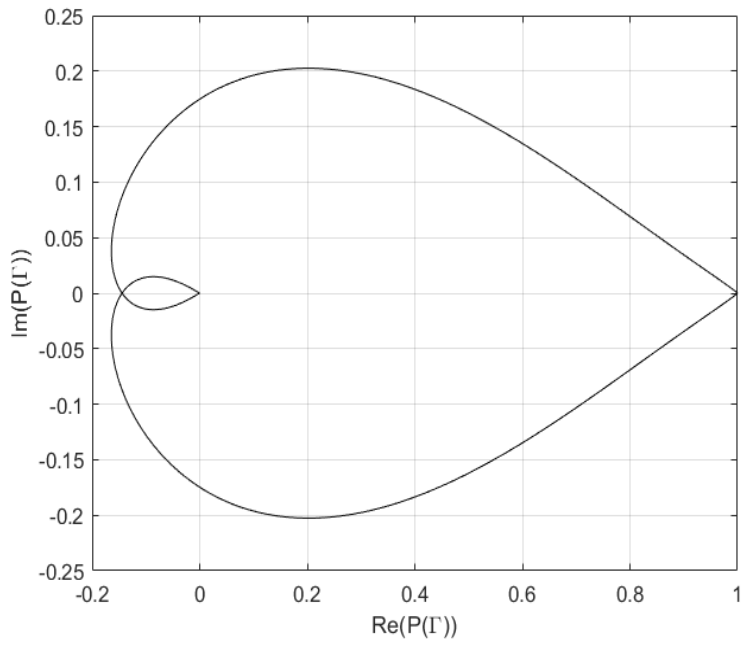
Figure 12: Example 3.3.2: $W(A(\Gamma), 0) = 2$.
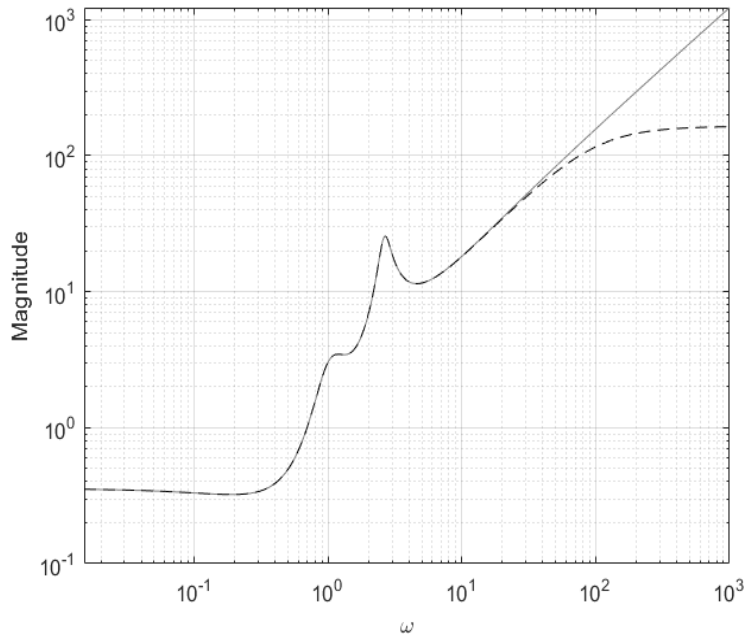

Figure 13: Example 3.3.2: Nyquist plot, P.

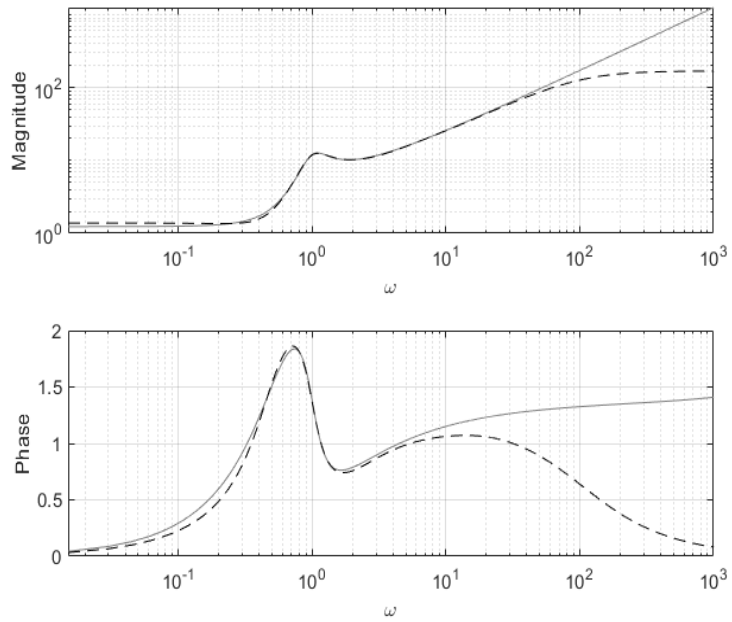Figure 14: Example 3.3.2: optimal Q (gray), rolled-off Q.

Figure 15: Example 3.3.2: optimal controller, C (gray), approximate rolled-off controller, $\tilde{C}$ (dashed).
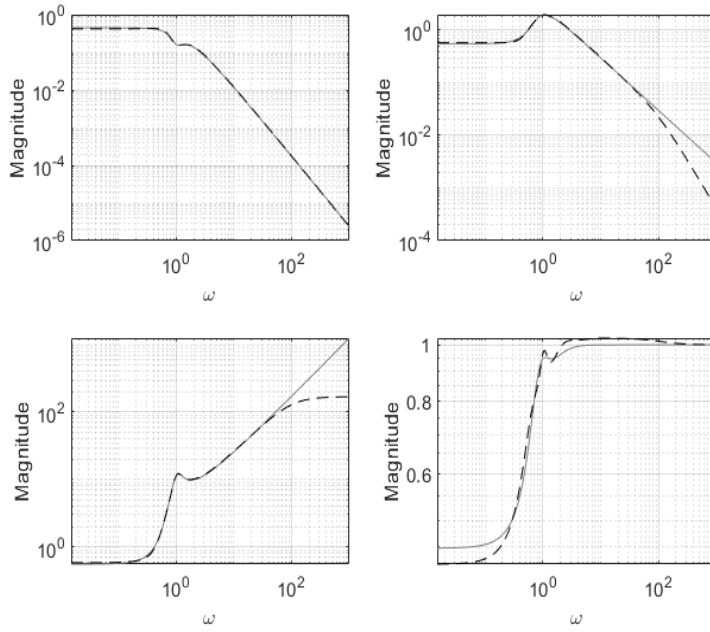
Figure 16: Example 3.3.2: optimal transfer functions, T_1 (upper left), T_2 (upper right), T_3 (bottom left), T_4 (bottom right), using C (gray), $\tilde{C}$ (dashed).
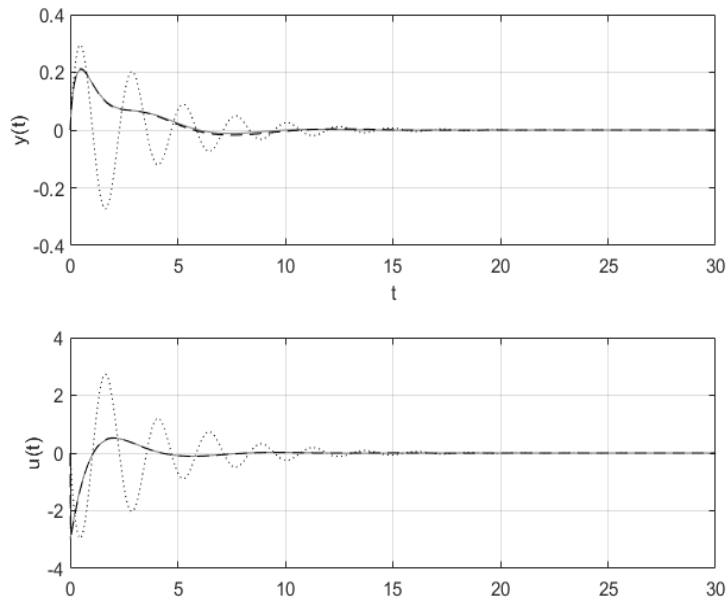

Figure 17: Example 3.3.2: optimal output, $y(t)$ (top), $u(t)$ (bottom), using C_0 (dotted), C (gray), $\tilde{C}$ (dashed).

4 Fractional LQR

The LQR is a benchmark problem commonly studied for its simple, elegant structure. Unlike the output feedback controller, which must reckon with only partial knowledge of the state, the LQR assumes full state feedback. Thus, the LQR describes the theoretically optimal behavior of a feedback control system when it has access to perfect information. However, fractional systems are infinite dimensional, so the definition of state feedback is ambiguous. For scalar fractional systems, we define a frequency domain analogy to state feedback, from which we develop the concept of the optimal feedback law in an operator theoretic sense.

4.1 Derivation of Optimal Feedback Law

For a general fractional differential equation (1), we can express $y(t)$ as a function of an internal state, $x(t)$, with input $u(t)$:

$$y(t) = \sum b_j \mathscr{D}^{\beta_j} x(t), \tag{189}$$

$$\sum a_i \mathscr{D}^{\alpha_i} x(t) = u(t). \tag{190}$$

In the frequency domain,

$$Y(s) = f_\beta(s)X(s) = \sum b_j s^{\beta_j} X(s), \tag{191}$$

$$f_\alpha(s)X(s) = \sum a_i s^{\alpha_i} X(s) = U(s), \tag{192}$$

where $\alpha = \max_i \alpha_i$ and $\beta = \max_j \beta_j$. We assume we have feedback of $X(s)$. We also assume $D(s)$ is an uncorrelated, impulsive disturbance. This configuration defines our notion of the fractional LQR with state feedback, as shown in Fig. 18.

The LQR problem, usually posed in the time domain, is to minimize J,

$$J = \int_0^\infty (\sum q_k \mathscr{D}^{\sigma_k} x(t))^2 + Ru(t)^2 dt, \tag{193}$$

where $q_k \in \mathscr{R}$, $\sigma_k \in \mathscr{R}^+$, and $R \in \mathscr{R}^+$. From Parseval's theorem [4],

$$J = \frac{1}{2\pi i} \int_{-i\infty}^{i\infty} |q(s)X(s)|^2 + R|U(s)|^2 ds, \tag{194}$$

where $q(s)$ is the fractional polynomial weighting the state,
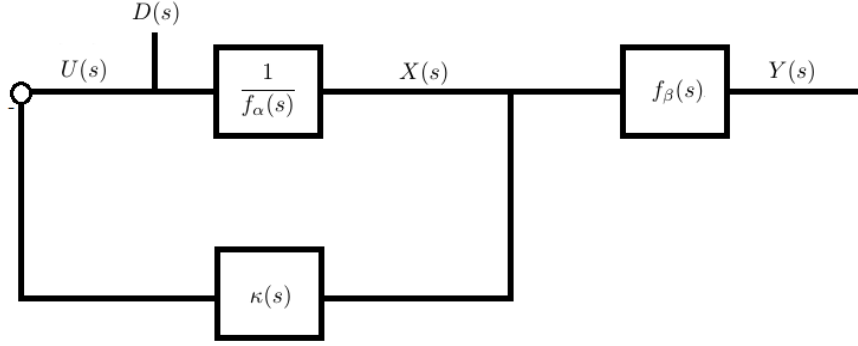
$$q(s) = \sum q_k s^{\sigma_k}. \tag{195}$$

41

Figure 18: Block diagram of regulator problem.

For instance, if $q(s) = 1$, then we penalize the state, $X(s)$, whereas if $q(s) = f_\beta(s)$, then we penalize the output, $Y(s)$.

We seek the optimal feedback law,

$$U = -\kappa X, \tag{196}$$

where

$$X = \frac{G}{1 + \kappa G} D, \tag{197}$$

$$G = \frac{1}{f_\alpha}. \tag{198}$$

We will assume $|D|^2 = 1$ since the spectrum of an uncorrelated, impulsive disturbance is a constant, and a constant will not affect the minimization procedure. This converts the LQR problem into a subset of the $\mathscr{H}_2$ problem,

$$\min_\kappa \left\| \frac{qG}{1 + \kappa G} \right\|^2 + R \left\| \frac{\kappa G}{1 + \kappa G} \right\|^2. \tag{199}$$

Because the assumption of state feedback circumvents the internal stability requirement, we are free to use the substitution,

$$\kappa = \frac{G - H}{GH}. \tag{200}$$

Thus, the cost function becomes

$$\min_H \|qH\|^2 + R \left\| \frac{H - G}{G} \right\|^2. \tag{201}$$

As we will show, the simplicity of this formulation grants a more explicit structure to the solution of the fractional LQR problem than that of the fractional $\mathscr{H}_2$ problem.

42

Because the cost function is quadratic in H, we can again use Wiener-Hopf spectral factorization. The optimal, stable H satisfies

$$\Omega^- = \frac{\partial}{\partial \bar{H}}\left(|qH|^2 + R\left|\frac{H-G}{G}\right|^2\right),\tag{202}$$

where Ω^- is unstable [4]. Hence,

$$\Omega^- = -R\bar{f}_\alpha + \gamma H,\tag{203}$$

where

$$\gamma = R|f_\alpha|^2 + |q|^2.\tag{204}$$

Given the factorization, $\gamma = \gamma^+\gamma^-$, and decomposition, $R\bar{f}_\alpha/\gamma^- = \{R\bar{f}_\alpha/\gamma^-\}_+ + \{R\bar{f}_\alpha/\gamma^-\}_-$,

$$\frac{\Omega^-}{\gamma^-} + \left\{\frac{R\bar{f}_\alpha}{\gamma^-}\right\}_- = -\left\{\frac{R\bar{f}_\alpha}{\gamma^-}\right\}_+ + \gamma H.\tag{205}$$

From analytic continuity,

$$H = \frac{1}{\gamma^+}\left\{\frac{R\bar{f}_\alpha}{\gamma^-}\right\}_+.\tag{206}$$

Comparing this result and the expression for Q (109), the formal similarity of the solutions is apparent.

The factorization, $\gamma = \gamma^+\gamma^-$, can obtained with Theorem 3.1. We now require the stable part of $R\bar{f}_\alpha/\gamma^- = \{R\bar{f}_\alpha/\gamma^-\}_+ + \{R\bar{f}_\alpha/\gamma^-\}_-$. Since all the roots and branch points of γ^- are unstable, $R\bar{f}_\alpha/\gamma^-$ has no stable poles or branch points whatsoever. This does not imply, however, that $\{R\bar{f}_\alpha/\gamma^-\}_+ = 0$. As $s \to \infty$,

$$\frac{R\bar{f}_\alpha}{\gamma^-} \to \frac{R(-s)^\alpha}{R^{\frac{1}{2}}(-s)^\alpha} = R^{\frac{1}{2}}.\tag{207}$$

In other words, $\mathscr{L}^{-1}(R\bar{f}_\alpha/\gamma^-)(t)$ approaches a delta function at $t = 0$, which is contained in the stable part. Thus,

$$\left\{\frac{R\bar{f}_\alpha}{\gamma^-}\right\}_+ = R^{\frac{1}{2}},\tag{208}$$

$$\left\{\frac{R\bar{f}_\alpha}{\gamma^-}\right\}_- = \frac{R\bar{f}_\alpha}{\gamma^-} - R^{\frac{1}{2}}.\tag{209}$$

Therefore, the optimal H is

$$H = \frac{R^{\frac{1}{2}}}{\gamma^+}.\tag{210}$$

Consequently, the optimal feedback law, κ, is

$$\kappa = R^{-\frac{1}{2}}\gamma^+ - f_\alpha.\tag{211}$$

4.2 Analysis of Optimal Feedback Law

We now analyze the meaning of the optimal feedback law, $U = -\kappa X$. The loop gain resulting from this feedback law is

$$L = \kappa G = \frac{R^{-\frac{1}{2}}\gamma^+ - f_\alpha}{f_\alpha}. \tag{212}$$

The square modulus of the return difference, $1 + L$, satisfies

$$|1 + L|^2 = \frac{|\gamma^+|^2}{R|f_\alpha|^2} = 1 + \frac{|q|^2}{R|f_\alpha|^2} \geq 1. \tag{213}$$

This implies that L obeys the *circle criterion*; in other words, L does not come within a unit circle centered around the -1 point on the Nyquist plot. This guarantees a gain margin, $0.5 < GM < \infty$, and phase margin, $|PM| \geq \pi/3$. This resemblance to the LQR is not accidental.

We restricted our design of the Wiener-Hopf regulator to impulsive plant disturbances, $D(s)$, with state penalty, $|q(s)X(s)|^2$. These conditions can be recognized as a subset of the standard LQR problem, where for a rational plant with state space representation, $\dot{\vec{x}}(t) = A\vec{x}(t) + Bu(t)$, we use the initial condition, $\vec{x}(0) = B$, with state penalty, $\vec{x}^T(t)Q\vec{x}(t)$, $Q \geq 0$ [17]. The loop gain can be expressed in terms of the elements, K_i, of the optimal gain matrix, K [17],

$$L(s) = K[sI - A]^{-1}B = \frac{\sum_{i=1}^n K_i s^{i-1}}{p_n(s)}, \tag{214}$$

where $p_n(s)$ is the characteristic polynomial. We can equate this expression to the loop gain that would be obtained by spectral factorization,

$$\frac{\sum_{i=1}^n K_i s^{i-1}}{p_n(s)} = \frac{R^{-\frac{1}{2}}\gamma^+(s) - p_n(s)}{p_n(s)}. \tag{215}$$

Comparing the numerators, we see that the expression, $R^{-\frac{1}{2}}\gamma^+ - p_n$, corresponds to a weighted sum of integer derivatives of $x(t)$, the coefficients of which are the optimal gains, K_i. Defining k as the optimal feedback polynomial,

$$k = R^{-\frac{1}{2}}\gamma^+ - p_n, \tag{216}$$

the meaning of the optimal feedback fractional polynomial, κ, becomes clear.

The optimal feedback law, $U(s) = -\kappa(s)X(s)$, is the fractional generalization of the notion of a weighted sum over derivatives of $x(t)$. Whereas the normal feedback law, $u(t) = -K\vec{x}(t) = -\mathscr{L}^{-1}(k(s)X(s))$, is a local

operation that sums only integer derivatives of the state, the fractional feedback law, $u(t) = -\kappa(t) * x(t) = -\mathscr{L}^{-1}(\kappa(s)X(s))$, is a non-local operation that sums over continuum of fractional derivatives of the state. Note that the optimal feedback law calculated in the time-domain does not depend on initial conditions. Consequently, neither does that resulting from the Wiener-Hopf method. Thus, $\kappa(s)$ is optimal for all initial conditions of the fractional system.
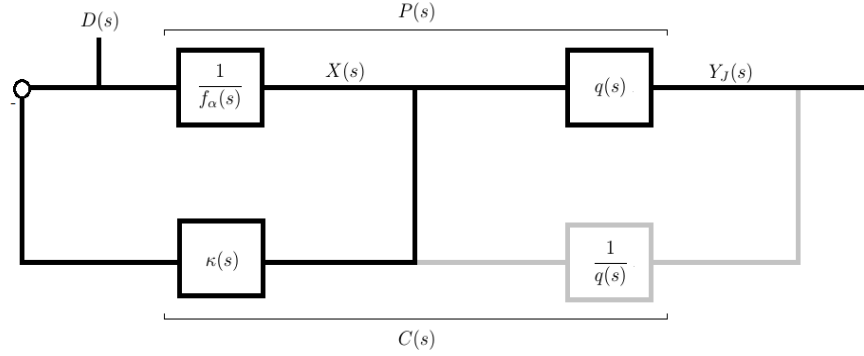

Figure 19: Transformation of full-state feedback regulator (black) to equivalent output feedback regulator (gray) for fractional system.
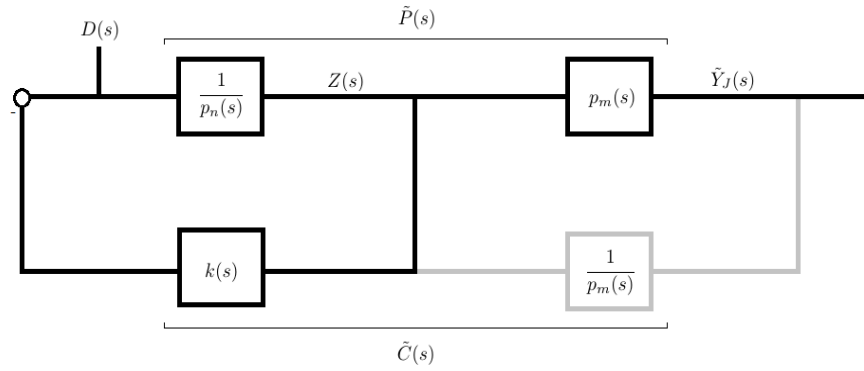

Figure 20: Transformation of equivalent output feedback regulator (gray) to full-state feedback regulator (black) for rational approximation of fractional system.

Though κ does not have an explicit fractional polynomial description, it is completely specified by its magnitude and phase. Nevertheless, one might wonder what the asymptotic growth rate of κ is. Comparing k and κ,

$$k = [|p_n|^2 + R^{-1}|q|^2]^+ - p_n, \tag{217}$$

45

$$\kappa = [|f_\alpha|^2 + R^{-1}|q|^2]^+ - f_\alpha, \tag{218}$$

we can at least reach an algebraic conclusion about the order of k. Because the s^n term is eliminated, the order of k depends on the second highest-order term in p_n, the s^{n-1} term. Hence, one might expect the order of κ to depend on the second highest-order term in f_α. Surprisingly, this is not the case. To see this, we recast the full-state feedback regulator problem as the fictitious output feedback problem shown in Fig. 19, with the internal stability requirement relaxed i.e. the output feedback controller may be improper or contain RHP pole-zero cancellations with the plant. With this configuration, we consider $Y_J = qX$ as the output and P as the transfer function:

$$P = \frac{q}{f_\alpha}. \tag{219}$$

Examining Fig. 19, the optimal but not realizable controller, C, that generates the same optimal control as the full-state feedback regulator is

$$C = \frac{\kappa}{q}. \tag{220}$$

We can interpret C as the series connection of the optimal feedback fractional polynomial, κ, and an observer, $1/q$, which perfectly reconstructs the internal state, X, from Y_J. Now, we construct an approximation of the fictitious output feedback system, shown in Fig. 20, by approximating P with an arbitrarily high order, rational, strictly proper, transfer function,

$$\tilde{P} = \frac{p_m}{p_n}, \tag{221}$$

such that $\tilde{P} \to P$ as $n > m \to \infty$. Note that any approximation scheme such that $\tilde{P} \to P$ is sufficient. Examining Fig. 20, the optimal but not realizable controller for this approximation, $\tilde{C}$, that generates the same optimal control as the full-state feedback regulator of the approximate system, is

$$\tilde{C} = \frac{k}{p_m}, \tag{222}$$

where $k = [|p_n|^2 + R^{-1}|p_m|^2]^+ - p_n$. As before, we can interpret $\tilde{C}$ as the series connection of the optimal feedback polynomial, k, and an observer, $1/p_m$, which perfectly reconstructs the internal state of the approximation, Z, from $\tilde{Y}_J$. Since $\tilde{Y}_J \to Y_J$ as $n > m \to \infty$, the approximate loop gain asymptotically approaches the fractional one,

$$\tilde{P}\tilde{C} \to PC. \tag{223}$$

46

Consequently, the asymptotic order of κ can be related to that of k,

$$\mathcal{O}\left(\frac{k}{p_n}\right) = \mathcal{O}\left(\frac{\kappa}{f_\alpha}\right). \tag{224}$$

Because $n > m$, k is a polynomial of order $n-1$. Therefore, κ, must satisfy

$$\mathcal{O}(\kappa) = \mathcal{O}(s^{\alpha-1}). \tag{225}$$

Evidently, the analogy between k and κ can be taken further. In the rational case, k sums over the first $n-1$ derivatives of the state and thus behaves as an $n-1$ order differentiator. In the fractional case, κ behaves as an $\alpha - 1$ order differentiator. This property holds regardless of lower order terms in f_α, which may even come within one order of α.

The interpretation of κ yields a simple interpretation of the optimal $\mathcal{H}_2$ controller, C, when the plant, P, is minimum phase. Using the parameterization, $C = (P - H)(PH)^{-1}$, the $\mathcal{H}_2$ problem becomes

$$\min_H \|H\|^2 + R\left\|\frac{H - P}{P}\right\|^2. \tag{226}$$

Proceeding as before,

$$\Omega^- = \frac{\partial}{\partial \bar{H}}\left(|H|^2 + R\left|\frac{H - P}{P}\right|^2\right), \tag{227}$$

where Ω^- is unstable. This yields

$$\Omega^- = -R\frac{\bar{f}_\alpha}{\bar{f}_\beta} + \frac{\gamma}{|f_\beta|^2}H. \tag{228}$$

After obtaining the factorization, $\gamma = \gamma^+\gamma^-$,

$$\frac{\Omega^-\bar{f}_\beta}{\gamma^-} + \left\{\frac{R\bar{f}_\alpha}{\gamma^-}\right\}_- = -\left\{\frac{R\bar{f}_\alpha}{\gamma^-}\right\}_+ + \frac{\gamma^+}{f_\beta}H. \tag{229}$$

Noting that the additive decomposition again reduces to a constant,

$$H = \frac{R^{\frac{1}{2}}f_\beta}{\gamma^+}. \tag{230}$$

Thus, the optimal output feedback controller is,

$$C = \frac{R^{-\frac{1}{2}}\gamma^+ - f_\alpha}{f_\beta} = \frac{\kappa}{f_\beta}. \tag{231}$$

Since $X = f_\beta^{-1}Y$ and $U = -\kappa X$, the output feedback controller can be interpreted as the series connection of an observer that perfectly reconstructs the state from the output and the optimal feedback fractional

47

polynomial that operates on the state. While C is improper and must be rolled off in practice, the ideal C can still be understood in this way.

4.3 Examples

In the following examples, we use spectral factorization to construct the optimal feedback law for fractional differential equations given full-state feedback.

4.3.1 Example

Consider the fractional differential equation,

$$\mathscr{D}^{\sqrt{13}}x(t) + \mathscr{D}^{3}x(t) - \mathscr{D}^{\sqrt{7}}x(t) + x(t) = u(t). \tag{232}$$

In the frequency domain, $f_{\sqrt{13}}(s)X(s) = U(s)$, where

$$f_{\sqrt{13}}(s) = s^{\sqrt{13}} + s^3 - s^{\sqrt{7}} + 1. \tag{233}$$

We choose a control weighting $R = 0.25$ and penalize $\mathscr{D}^{\sqrt{3}}x(t) + x(t)$ by choosing

$$q(s) = s^{\sqrt{3}} + 1. \tag{234}$$

To calculate κ, we require the stable multiplicative factor of $\gamma = \gamma^{+}\gamma^{-}$ where from (204),

$$\gamma = 0.25|f_{\sqrt{13}}|^2 + |q|^2. \tag{235}$$

To effect this factorization, we require an appropriate reference function, $\lambda = \lambda^{+}\lambda^{-}$.

Noting that $g(s) = 0.5(s^{\sqrt{13}} + s^3 - s^{\sqrt{7}} + 10s^{\sqrt{3}} + 11)$ is stable (see Example 3.3.2), we choose $\lambda = |g|^2$ and calculate γ^{+} with Theorem 3.1. From (211), the optimal feedback fractional polynomial is

$$\kappa(s) = [|f_{\sqrt{13}}|^2 + 4|q|^2]^{+} - f_{\sqrt{13}}. \tag{236}$$

From (212), the resulting loop gain is

$$L(s) = \frac{[|f_{\sqrt{13}}|^2 + 4|q|^2]^{+} - f_{\sqrt{13}}}{f_{\sqrt{13}}}. \tag{237}$$

The optimal feedback law satisfies $\mathscr{O}(\kappa) = \mathscr{O}(s^{\sqrt{13}-1})$, as shown in Fig. 21. Moreover, L obeys the circle criterion (213), as shown in Fig. 22.

We compare the results here to the optimal output feedback controller, C, for the plant in Example 3.3.2. Because the plant is minimum phase, we can interpret C as the series connection of κ and an observer, $1/f_{\sqrt{3}}$:

$$C = \frac{\kappa}{f_{\sqrt{3}}}. \tag{238}$$

The state, $X(s)$, is reconstructed from the output, $Y(s)$, by the observer, $1/f_{\sqrt{3}}$. The optimal control is then generated by fractionally differentiating $X(s)$ with the optimal control law, κ. This interpretation is verified in Fig. 23.
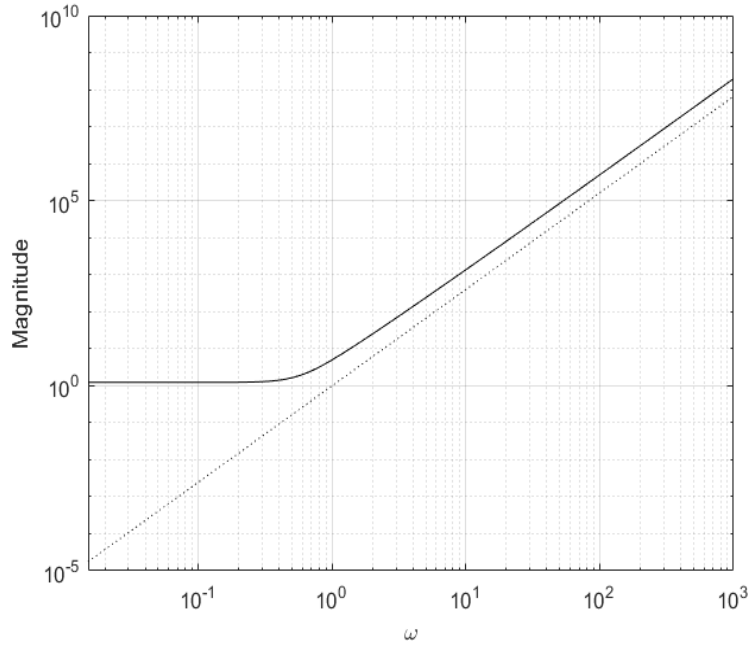
Figure 21: Example 4.3.1: optimal feedback fractional polynomial, κ (solid), $s^{\sqrt{13}-1}$ (dotted).

4.3.2 Example

Consider the fractional differential equation,

$$8\mathscr{D}^{\sqrt{8}}x(t) + 6\mathscr{D}^{\sqrt{6}}x(t) + 5\mathscr{D}^{\sqrt{5}}x(t) + 3\mathscr{D}^{\sqrt{3}}x(t) + 2\mathscr{D}^{\sqrt{2}}x(t) - x(t) = u(t). \tag{239}$$

In the frequency domain, $f_{\sqrt{8}}(s)X(s) = U(s)$, where

$$f_{\sqrt{8}}(s) = 8s^{\sqrt{8}} + 6s^{\sqrt{6}} + 5s^{\sqrt{5}} + 3s^{\sqrt{3}} + 2s^{\sqrt{2}} - 1. \tag{240}$$
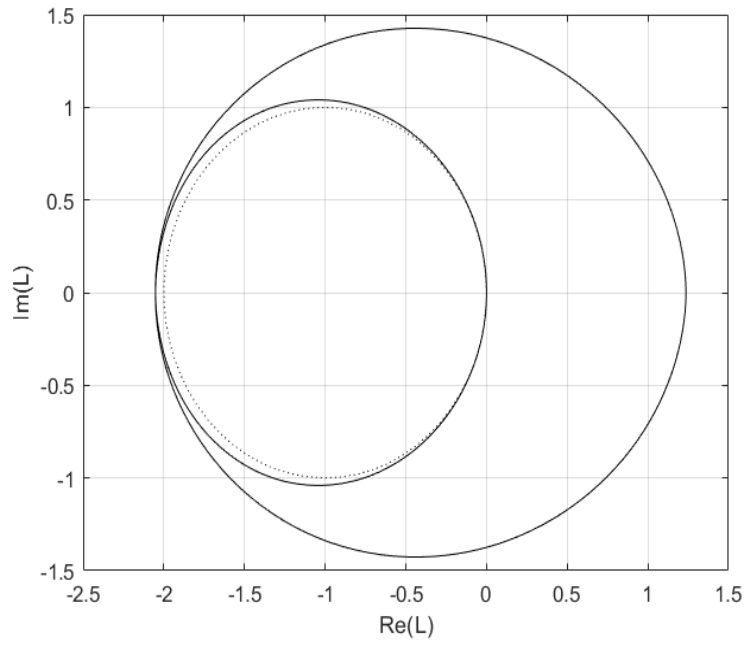
49

Figure 22: Example 4.3.1: loop gain, L (solid), unit circle centered on -1 (dotted).
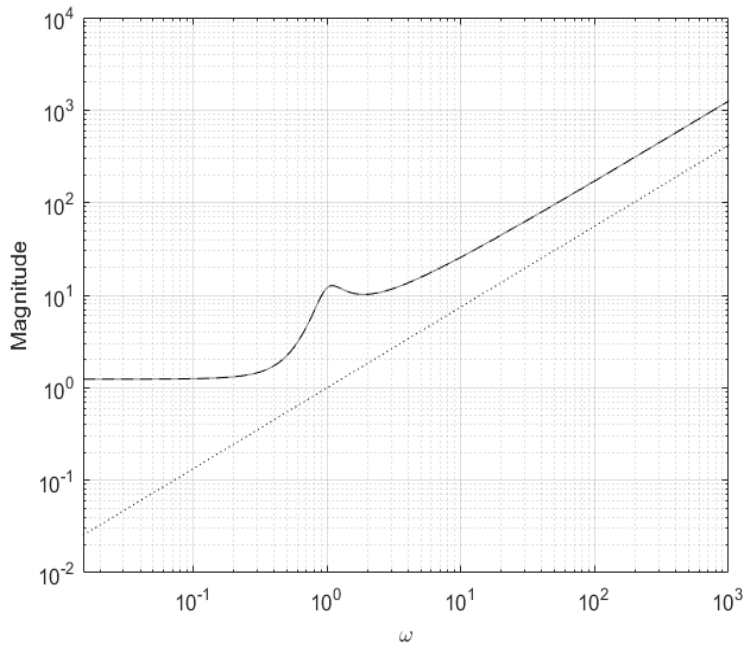

Figure 23: Example 4.3.1: optimal controller, C (gray solid), $\kappa/f_{\sqrt{3}}$ (dashed), $s^{\sqrt{13}-1-\sqrt{3}}$ (dotted).

Defining the normalized transfer function,

$$A(s) = \frac{f_{\sqrt{8}}(s)}{(s^{\sqrt{8}/2} + 1)^2}, \tag{241}$$

we can see from Fig. 24 that $f_{\sqrt{8}}$ is unstable.

We choose a control weighting $R = 4$ and penalize $\dot{x}(t) + x(t)$ by choosing

$$q(s) = s + 1. \tag{242}$$

To calculate κ, we require the stable multiplicative factor of $\gamma = \gamma^+ \gamma^-$ where from (204),

$$\gamma = 4|f_{\sqrt{8}}|^2 + |q|^2. \tag{243}$$

To effect this factorization, we require an appropriate reference function, $\lambda = \lambda^+ \lambda^-$.

From Corollary 3.1.1,

$$g(s) = \frac{2(s^{\sqrt{5}/2} + 1)^2 (8s^{\sqrt{8}} + 6s^{\sqrt{6}} + 5s^{\sqrt{5}})}{s^{\sqrt{5}}}, \tag{244}$$

is stable. We choose $\lambda = |g|^2$ and calculate γ^+ with Theorem 3.1. From (211), the optimal feedback fractional polynomial is

$$\kappa(s) = [|f_{\sqrt{8}}|^2 + 0.25|q|^2]^+ - f_{\sqrt{8}}. \tag{245}$$

From (212), the resulting loop gain is

$$L(s) = \frac{[|f_{\sqrt{8}}|^2 + 0.25|q|^2]^+ - f_{\sqrt{8}}}{f_{\sqrt{8}}}. \tag{246}$$

The optimal feedback law satisfies $\mathscr{O}(\kappa) = \mathscr{O}(s^{\sqrt{8}-1})$, as shown in Fig. 25. Moreover, L obeys the circle criterion (213), as shown in Fig. 26.

4.3.3   Example

Consider the fractional differential equation,

$$\mathscr{D}^{\sqrt{6}}x(t) - \mathscr{D}^{\sqrt{5}}x(t) + \mathscr{D}^2 x(t) - \mathscr{D}^{\sqrt{3}}x(t) + \mathscr{D}^{\sqrt{2}}x(t) + 10x(t) = u(t). \tag{247}$$

In the frequency domain, $f_{\sqrt{6}}(s)X(s) = U(s)$, where

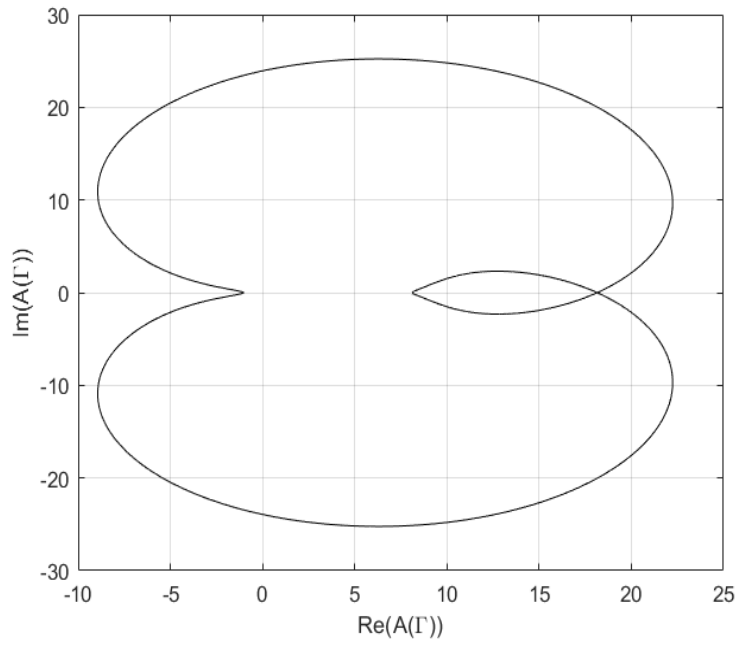$$f_{\sqrt{6}}(s) = s^{\sqrt{6}} - s^{\sqrt{5}} + s^2 - s^{\sqrt{3}} + s^{\sqrt{2}} + 10. \tag{248}$$

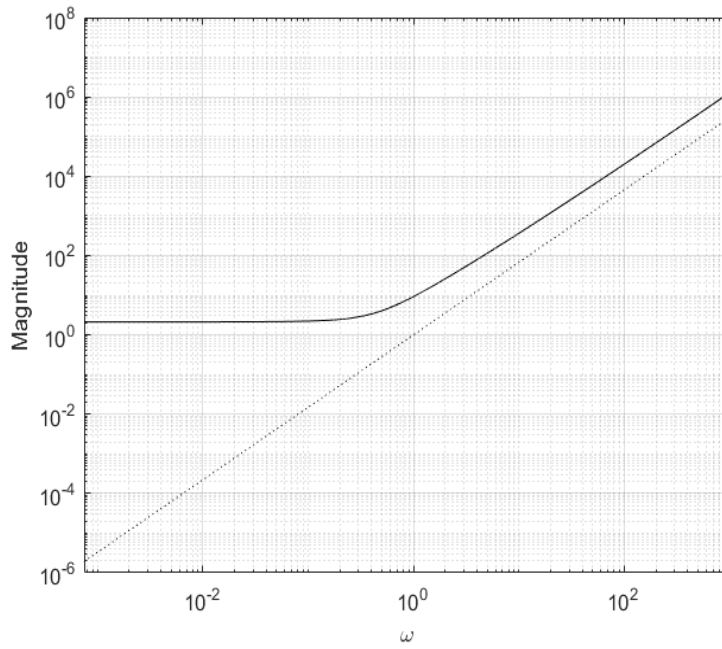Figure 24: Example 4.3.2: $W(A(\Gamma), 0) = 1$.

Figure 25: Example 4.3.2: optimal feedback fractional polynomial, κ (solid), $s^{\sqrt{8}-1}$ (dotted).
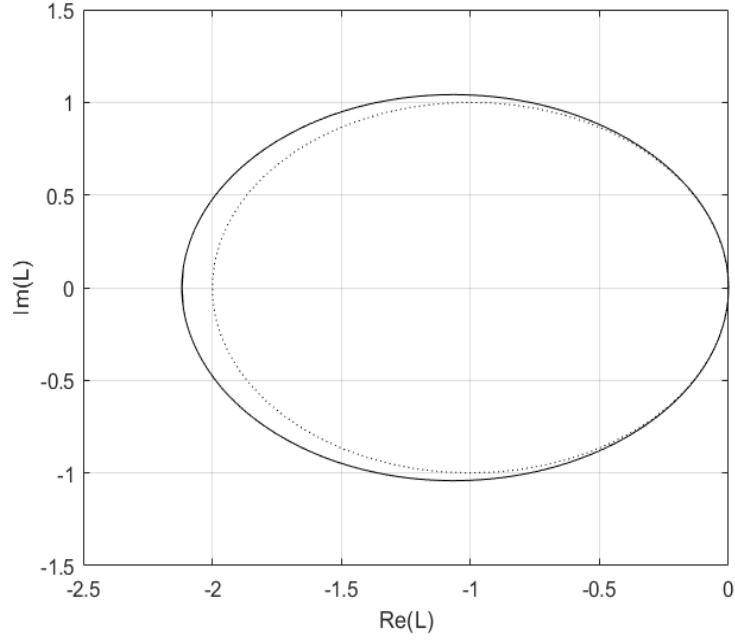
Figure 26: Example 4.3.2: loop gain, L (solid), unit circle centered on -1 (dotted).

Defining the normalized transfer function,

$$A(s) = \frac{f_{\sqrt{6}}(s)}{(s^{\sqrt{6}/2} + 1)^2}, \tag{249}$$

we can see from Fig. 24 that $f_{\sqrt{6}}$ is unstable.

We choose a control weighting $R = 0.25$ and penalize $\dot{x}(t)$ by choosing

$$q(s) = s. \tag{250}$$

To calculate κ, we require the stable multiplicative factor of $\gamma = \gamma^+\gamma^-$ where from (204),

$$\gamma = 0.25|f_{\sqrt{6}}|^2 + |q|^2. \tag{251}$$

To effect this factorization, we require an appropriate reference function, $\lambda = \lambda^+\lambda^-$.

Picking the stable polynomial, r,

$$r(s) = s + 1, \tag{252}$$

we construct the stable fractional polynomial,

$$f_{\sqrt{6}} + 5r, \tag{253}$$

53

using the Nyquist plot, as shown in Fig. 28. We choose $\lambda = |0.5(f_{\sqrt{6}} + 5r)|^2$ and calculate γ^+ with Theorem 3.1. From (211), the optimal feedback fractional polynomial is

$$\kappa(s) = [|f_{\sqrt{6}}|^2 + 4|q|^2]^+ - f_{\sqrt{6}}. \tag{254}$$

From (212), the resulting loop gain is

$$L(s) = \frac{[|f_{\sqrt{6}}|^2 + 4|q|^2]^+ - f_{\sqrt{6}}}{f_{\sqrt{6}}}. \tag{255}$$

The optimal feedback law satisfies $\mathscr{O}(\kappa) = \mathscr{O}(s^{\sqrt{6}-1})$, as shown in Fig. 29. Moreover, L obeys the circle criterion (213), as shown in Fig. 30.
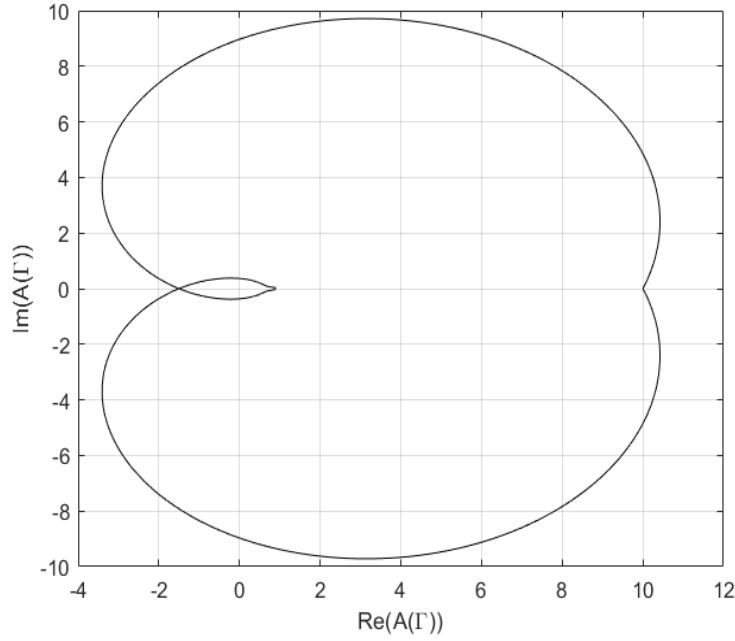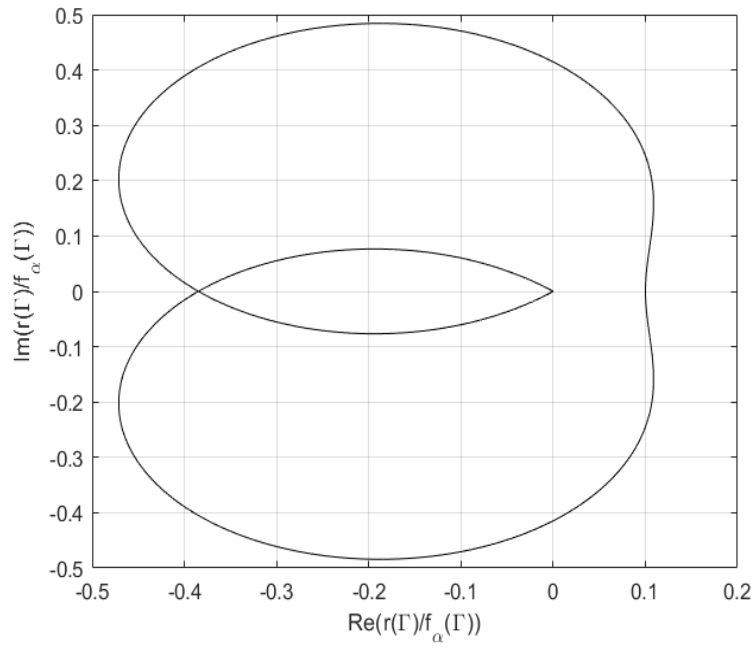

Figure 27: Example 4.3.3: $W(A(\Gamma, 0) = 2$.
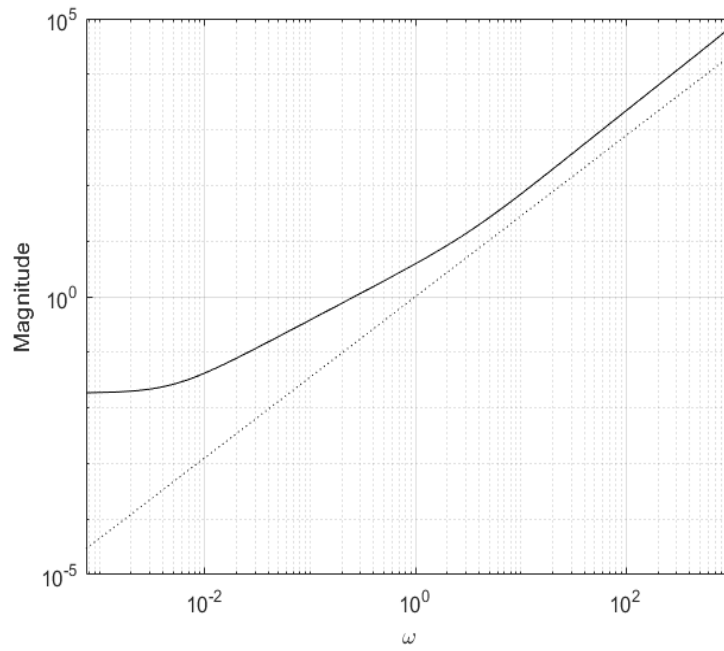
Figure 28: Example 4.3.3: Nyquist plot, $r/f_{\sqrt{6}}$.

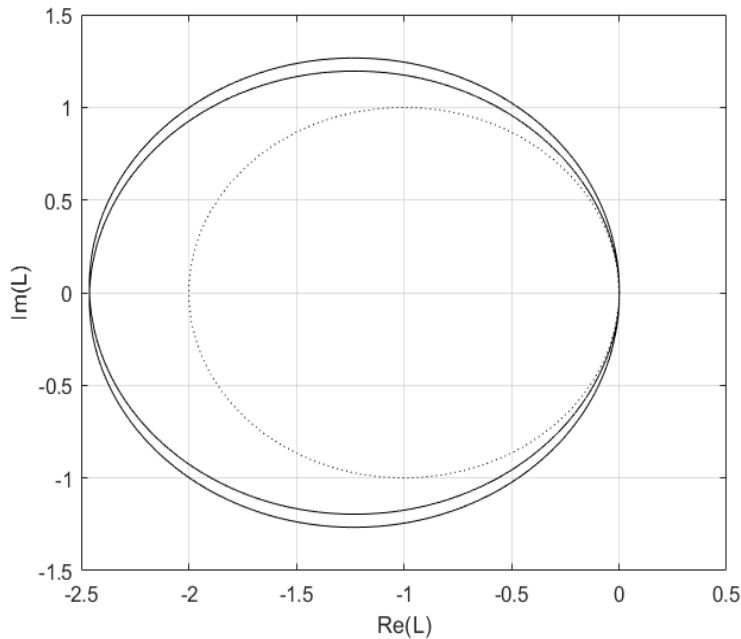Figure 29: Example 4.3.3: optimal feedback fractional polynomial, κ (solid), $s^{\sqrt{6}-1}$ (dotted).

55

Figure 30: Example 4.3.3: loop gain, L (solid), unit circle centered on -1 (dotted).

5   Conclusion

We have solved the scalar $\mathscr{H}_2$ and LQR problem for fractional systems with spectral factorization. To do so, we derived several useful theorems regarding the location and number of roots of fractional polynomials. We explained the use of the Argument Principle and root locus on the slit s-plane when obtaining stabilizing controllers. We then constructed the fractional order Youla parameterization from knowledge of a nominal stabilizing controller. This parameterization allowed us to linearize the closed-loop sensitivity functions while preserving internal stability. We then reduced the fractional $\mathscr{H}_2$ problem to a Wiener-Hopf spectral factorization problem. In order to obtain the key product decomposition, we used an integral factorization technique, which required careful selection of a reference function to ensure convergence of the relevant integrals. From this we constructed the optimal output feedback controller. Finally, we used the integral factorization technique to solve the fractional LQR problem using a frequency domain notion of state feedback. We found that the fractional optimal feedback law corresponded to an $\alpha - 1$ order differentiator operating on the state, analogous to interpreting the optimal gains for a rational system as a weighted sum of $n - 1$ derivatives of the state.

The extension to multiple-input, multiple-output fractional systems is non-trivial. Recall that in the scalar case, we reduced the product decomposition to an additive decomposition using the logarithm (see Section 3.2). To convert the additive decomposition back to the product decomposition, we relied on the property that

$$\exp(\Phi_+ + \Phi_-) = \exp\Phi_+ \exp\Phi_-. \tag{256}$$

In the matrix case, however,

$$\exp(\Phi_+ + \Phi_-) \neq \exp\Phi_+ \exp\Phi_-, \tag{257}$$

unless Φ_+ and Φ_- commute. It has been proven for arbitrary matrix kernels that these commuting factors do indeed exist [1]. However, it is unknown how to obtain these commuting factors except for certain special matrix kernels occuring in partial differential equations [1]. Without a matrix integral factorization technique, an element-wise plant approximation such as the Padé approximant used in [1] appears to be the only resort.

References

[1] I. D. Abrahams, *On the solution of Wiener-Hopf problems involving noncommutative matrix kernel decompositions*, SIAM Journal of Applied Math, 57, 1997.

[2] C. Bonnet and J. R. Partington, Coprime Factorizations and Stability of Fractional Differential Systems, *Systems & Control Letters*, 2000.

[3] J. W. Brown and R. V. Churchill, *Complex Variables and Applications*, New York: McGraw Hill, 7th ed., 2004.

[4] S. S. L. Chang, *Synthesis of Optimum Control Systems*, New York: McGraw Hill, 1st ed., 1961.

[5] S. S. L. Chang, *An extension of the initial value theorem and its application to random signal analysis*, Proc. IEEE (Letters), 56, 1968, p. 764.

[6] J. Doyle, B. A. Francis, and A. Tannenbaum. *Feedback Control Theory*, Macmillan Publishing Co., 1990.

[7] B. A. Francis, *On the Wiener-Hopf approach to optimal feedback design*, Systems & Control Letters, 1982.

[8] G. F. Franklin, J. D. Powell, and A. Emami-Naeini. *Feedback Control of Dynamic Systems*, New Jersey: Pearson Higher Education, Inc., 6th ed., 2010.

[9] H. Garnier, M. Mensler, and A. Richard, *Continuous-time model identification from sampled data: implementation issues and performance evaluation*, International Journal of Control, 76, 2003.

[10] C. A. Monje, Y. Chen, B. M. Vinagre, D. Xue, and V. Feliu, *Fractional-order Systems and Controls*, New York: Springer, 2010.

[11] B. Noble, *Methods Based on the Wiener-Hopf Technique for the Solution of Partial Differential Equations*, New York: Pergammon Press, 1st ed., 1958.

[12] F. Padula, S. Alcantara, R. Vilanova, and A. Visioli, $\mathscr{H}_\infty$ *control of fractional linear systems.*, Automatica, 49, 2013.

[13] D. Pierre, *Optimization Theory with Applications*, New York: John Wiley & Sons, Inc., 1st ed., 1969.

[14] I. Podlubny, *Fractional Differential Equations*, San Diego: Academic Press, 1999.

[15] M. Vidyasagar, Control System Synthesis: A Factorization Approach, The MIT Press, 1985.

[16] B. M. Vinagre and V. Feliu, *Optimal fractional controllers for rational order systems: a special case of the Wiener-Hopf spectral factorization method*, IEEE Transactions on Automatic Control, 52, 2007.

[17] B. H. Willis and R. W. Brockett, *The frequency domain solution of regulator problems*, IEEE Transactions on Automatic Control, 10, 1965.

[18] D. C. Youla, *Modern Wiener-Hopf design of optimal controllers*, IEEE Transactions on Automatic Control, 21, 1976.